INSTITUTE OF PHYSICS PUBLISHING PHYSICS IN MEDICINE AND BIOLOGY

Phys. Med. Biol. **51** (2006) R455–R489 doi:10.1088/0031-9155/51/13/R25

REVIEW

Review of electron beam therapy physics

Kenneth R Hogstrom[1,2,3] **and Peter R Almond**[3]

[1] Department of Physics and Astronomy, Louisiana State University, 202 Nicholson Hall, Baton Rouge, LA 70803-4001, USA
[2] Mary Bird Perkins Cancer Center, 4950 Essen Lane, Baton Rouge, LA 70809-3482, USA
[3] Department of Radiation Physics, The University of Texas M D Anderson Cancer Center, 1515 Holcombe Boulevard, Houston, TX 77030-4009, USA

E-mail: hogstrom@lsu.edu

Received 14 March 2006, in final form 9 May 2006
Published 20 June 2006
Online at stacks.iop.org/PMB/51/R455

Abstract

For over 50 years, electron beams have been an important modality for providing an accurate dose of radiation to superficial cancers and disease and for limiting the dose to underlying normal tissues and structures. This review looks at many of the important contributions of physics and dosimetry to the development and utilization of electron beam therapy, including electron treatment machines, dose specification and calibration, dose measurement, electron transport calculations, treatment and treatment-planning tools, and clinical utilization, including special procedures. Also, future changes in the practice of electron therapy resulting from challenges to its utilization and from potential future technology are discussed.

Contents

1. Introduction

For over 50 years, electron beam therapy has been an important radiation therapy modality. A single electron beam delivers a uniform 'plateau' of dose ranging from 90% to 100% of maximum central-axis dose with the dose distribution steeply falling off both laterally and distally (cf figure 1(a)). This has allowed superficial cancers and disease (within 6 cm of the patient's surface) to be irradiated with little dose to underlying normal tissues and structures, something usually not possible with x-ray therapy. At beam energies greater than approximately 20 MeV, depth–dose curves lose their sharp fall-off and begin taking on characteristics of photon beams due to bremsstrahlung energy loss, whereas their penumbrae broaden with depth, due to increased multiple Coulomb scattering (cf figure 1(b)). Hence, accelerators having energies much greater than 20 MeV have yet to have a significant impact. The present review will therefore focus primarily on electron beams in the range of approximately 6–20 MeV, which are used to treat skin and superficial disease.

The purpose of this review is to identify the electron beam physics and dosimetry contributions that have had the most impact on patient treatment. Thousands of outstanding publications have been published on this topic, and deciding which ones to select for this review was difficult, so the authors apologize to those whose works are not mentioned but remain worthwhile. It is hoped that this review will place in perspective the history of important contributions of medical physics to electron beam therapy and will provide a door through which medical physicists new to the field of electron beam therapy can find useful information to further their knowledge of the field.

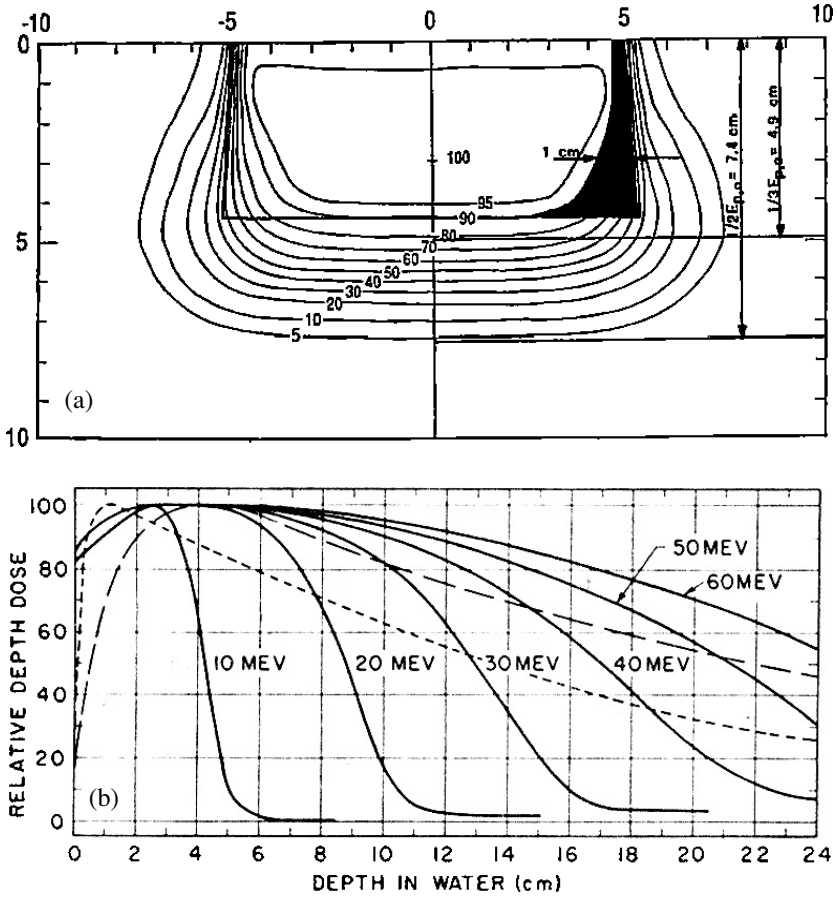

Figure 1. (a) Plot of isodose curves in water for a 15 MeV electron beam, 10 × 10 cm^2 field at 100 cm SSD. Lateral and distal dose fall-off, largely due to multiple Coulomb scattering, determines the minimum margin between tumour and protected normal tissue and between tumour and beam edge (from Hogstrom (1991)). (b) Depth–dose curves in water for multiple electron beam energies, 10–60 MeV (solid curves), for large fields at 200 cm SSD, are compared to depth–dose curves for 5 MV (small-dashed line) and 22 MV (long-dashed line) x-ray beams for a 10 × 10 cm^2 field at 100 cm SSD (from Loevinger *et al* (1961)).

2. Treatment machines

In the late 1930s and the early 1940s, the development of the Van de Graaff and betatron accelerators made possible megavoltage radiation therapy. The Van de Graaff generator was one of the first machines used for electron beam radiation therapy as reported by Trump (1964). These accelerators were limited, however, to a few MeV, and the electron beam could only be used to treat surface lesions. Betatrons, on the other hand, were able to accelerate electrons up to tens of MeV, which was useful in producing megavoltage x-ray beams that were of great interest for radiation therapy. The betatron became the accelerator of choice after World War II. Besides producing high-energy x-ray beams, they were able to produce electron beams in the energy range of 5 to approximately 30 MeV, which were also useful for radiation therapy. Pioneering work in the therapeutic use of high-energy electrons was primarily done

in Germany with a 6 MeV betatron developed by Gund and Paul (1950). A review of early investigations of higher energy electrons (6–22 MeV) was given by Laughlin *et al* (1953). During the same time period, electron linear accelerators were being developed using the microwave sources used in radar systems. Although the linear accelerator is inherently better suited to production of electron beams and some initial work had been done with them, e.g., the report by Loevinger and colleagues documenting the use of 6–60 MeV electron beams (Loevinger *et al* 1961), betatrons were less complex and less expensive, and most of the early clinical and radiologic physics studies were carried out using them (Markus 1978). By 1968, there were 137 clinical betatrons in use worldwide compared to 79 linear accelerators, but only a small fraction of these were capable of producing clinical electron beams. This can be compared to 20 Van de Graaff machines and 1676 Co-60 units, none of which were used for electron beam therapy (IAEA 1968).

The betatron uses electromagnetic induction to accelerate the electrons, and the inherent magnet field makes it difficult to extract the electron beams in a straight path. Care had to be taken, therefore, to obtain clinically useful electron beams, especially with respect to dose distribution (Gund and Paul 1950, Laughlin *et al* 1953). The machines were also quite large (the magnet for an 18 MeV betatron weighed about 400 kg, and the weight increased approximately with the cube of the electron energy) and noisy and often had a limited dose rate. The betatrons could, however, produce electron beams over a wide and selectable energy range (from around 5 MeV to the maximum machine energy of 20–42 MeV), with a very small energy spread. Much of the early physics and clinical studies were performed on these machines, including scattering foil design, calibration procedures, dose measurement and collimator design.

As linear accelerators developed, they gradually became the equipment of choice. Initially, various approaches were investigated to meet the different requirements of electron beam therapy. In order to produce large flat electron beam fields, various scanning techniques (Aucouturier *et al* 1970) were developed along with improvements to the scattering foil systems, which had been developed for use with the betatrons (e.g., Kozlov and Shishov (1976)). Today, sophisticated dual-foil scattering systems are used (Grusell *et al* 1994). These systems maximize the flattened field size with minimal production of bremsstrahlung and a minimal increase in energy spread (Green 1991, Klein *et al* 1995). Variable field-size collimators were developed and used on commercial machines, but the constraints on the design of such collimators have resulted in fixed field-size applicators, with secondary blocking being the standard on all present equipment.

The early accelerating structures were often several metres in length, and in order to have the treatment head rotate 360° (or as close to 360° as possible) around the patient, various approaches were attempted. Horizontal stationary structures with rotating magnetic-beam transport systems, vertical structures mounted on dual gantries and rotating horizontal structures were all attempted. All of these resulted in large, bulky machines, often with additional rooms required for the power supplies, modulators and associated electronics. However, improvements in the accelerating structures, modern electronics, computer control, bending magnet technology and a decrease in maximum beam energy to approximately 20 MeV have resulted in relatively compact machines that can be rotated fully around the patient and that require little or no space other than the treatment room.

In addition to linear accelerators, microtrons were also built for radiation therapy purposes. A single magnet microtron was developed in which the electron beam was accelerated by being repeatedly passed through a microwave resonant cavity to obtain the desired energy. A racetrack microtron, which used a short section of a linear accelerator structure through which the beam passed multiple times and was bent into a racetrack configuration by two magnets,

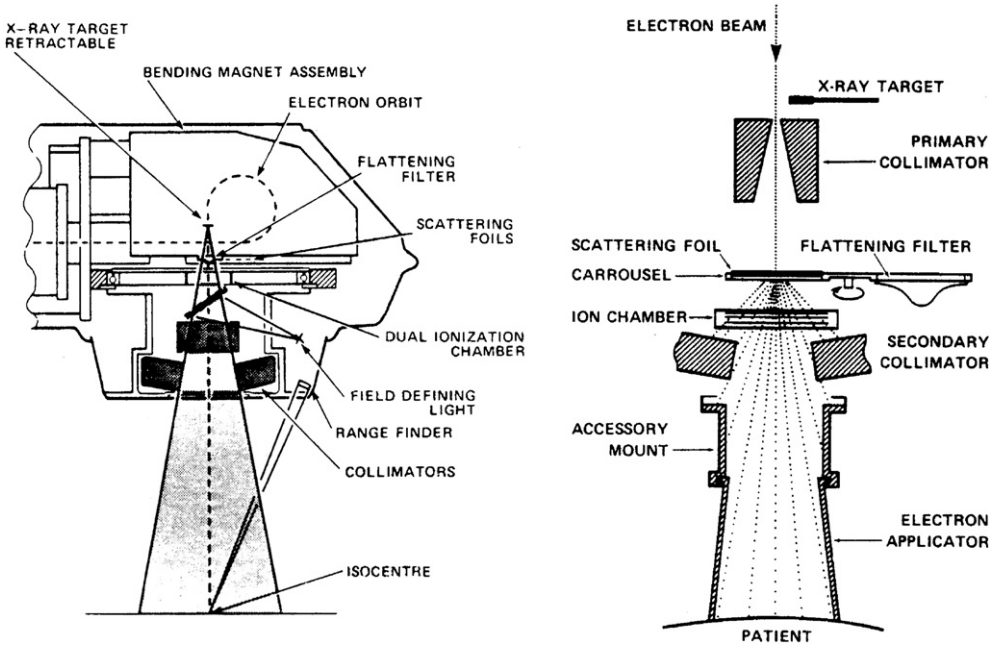

Figure 2. (a) Schematic view of modern day treatment head configuration. Note the 270° achromatic bending magnet that redirects the electron beam towards the patient. (b) Schematic view of treatment head configured for electron beam delivery. Note the scattering foil (actually dual-scattering foils separated 5–10 cm) to broaden the beam, secondary (x-ray) collimator and electron applicator to collimate the beam and ion chamber (actually dual, segmented ionization chamber) used to monitor the beam (from Karzmark and Morton (1989)).

has also been used (Brahme and Reistad 1981). A good summary of the accelerators used for producing fast electron beams is given by Klevenhagen (1985).

The major developments in microwave-based accelerators for electron beam therapy took place primarily after 1970. The treatment machines in use today are S-band linear accelerators, which are designed to produce both x-rays and electron beams. Because of the need to have a range of electron beam energies from approximately 6 to 20 MeV available in one machine, the linear accelerators used for electron beam therapy will also be the machines that are used for high-energy x-ray therapy (approximately 15–20 MV; they will generally also have a lower energy x-ray beam available). Although there is some variation in design between the various manufacturers, such as standing-wave or travelling-wave accelerating structures, side coupled cavities or not, magnetron or klystron machines, differences in beam-transport systems (i.e., bending magnet design), etc, all systems have a treatment head that consists of a number of important assemblies associated with directing, broadening, flattening, collimating and monitoring the beam (cf figure 2).

In addition to the machines used for routine clinical electron beam therapy, a few specialty machines have been built primarily for intraoperative therapy. These machines have either been installed in surgical suites or are mobile and can be moved into the operating room when needed. The former have been standard S-band linear accelerators without x-ray capabilities (Rich and Dally 1985) and the latter have been smaller X-band machines (Meurk *et al* 1997, Mills *et al* 2001, Beddar and Krishnan 2005).

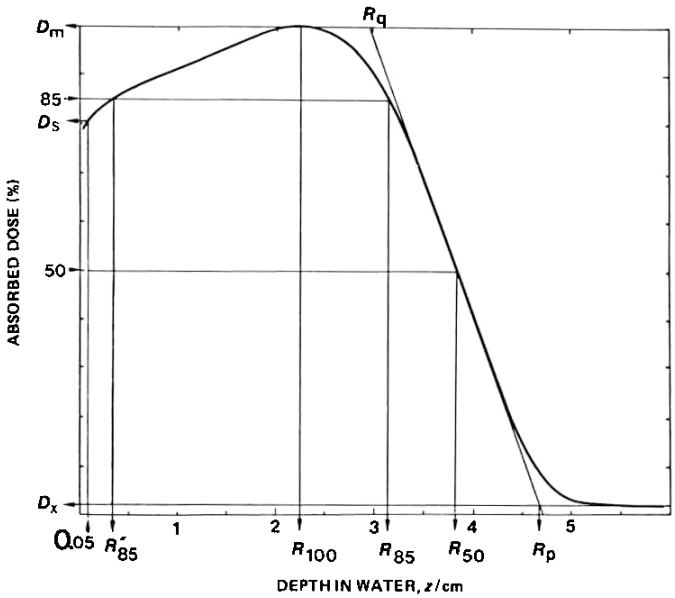

Figure 3. Specification of parameters used to characterize electron beam central-axis depth–dose curve. (1) The relative surface dose at 0.5 mm, $\%D_s$. Due to the difficulty of determining the dose at the surface, the relative surface dose is defined at a depth of 0.5 mm. (2) The relative dose due to the x-ray component, $\%D_x$. This should be as low as possible. (3) The therapeutic range, R_t, is a measure of the clinically useful portion of the depth–dose profile and is usually taken as the deepest 90% dose level. Historically, however, the therapeutic dose specification has varied between the 80% and 90% dose levels. (4) Range parameters R_{100}, R_{50} and R_p are the depth of the dose maximum, D_{max}, in water, the depth of the 50% dose level and the practical range, respectively. R_{50} and R_p are used in range energy equation. (5) R_q is the depth at which the tangent to the depth–dose curve at the point of inflection meets the level of D_{max}. (6) G_0, the normalized dose gradient, is a measure of the steepness of the descending portion of the depth–dose curve, $G_0 = R_p/(R_p - R_q)$. In general, a rapid fall-off of the dose beyond the therapeutic range is desirable (from ICRU (1984)).

3. Dose specification and calibration

3.1. Per cent depth dose specification

In selecting the appropriate electron beam energy to be used for a specified clinical case, the first consideration is matching the central-axis depth–dose curve parameters to the clinical situation. In accordance with ICRU 35 (1984), several parameters are used to characterize the electron beam central-axis depth–dose curve. Each of these parameters ($\%D_s$, $\%D_x$, R_t, R_{100}, R_{50}, R_p and G_0; defined in figure 3) is of clinical importance and can be affected by small differences in energy, scattering foils, collimation and source-to-surface distance (SSD). During acceptance-testing procedures, the central-axis depth–dose curves should be evaluated and compared to the specifications and adjustments to the beam energy made if necessary. Electron depth–dose curves also depend on the size and shape of the treatment field and will also change with energy as discussed by Brahme and Svensson (1976). As the energy increases, the changes in the central-axis depth–dose curve with field size become more pronounced (cf figure 4(a)) (Meyer *et al* 1984, van de Geijn *et al* 1987, ICRU 1984). Hogstrom *et al* (1981) showed that the central-axis depth–dose curve for rectangular fields of size X and Y can be determined using the square-root method, that is by taking the square root

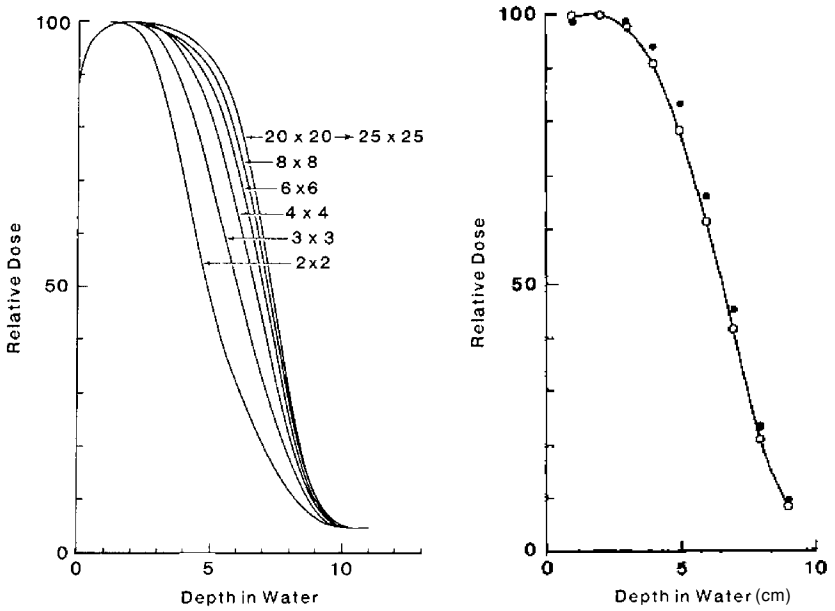

Figure 4. (a) The field-size dependence of per cent depth dose is illustrated for an 18 MeV beam. (b) For rectangular fields, per cent depth dose is best determined using the square-root method of Hogstrom *et al* (1981) (open circles) than by the equivalent-square method used for photon beams (closed circles); solid line is measured data for an 18 MeV beam, 3×8 cm^2 field size at 100 cm SSD (from Meyer *et al* (1984)).

of the product of the depth doses for the square fields whose sides are X and Y (cf figure 4(b)). Computer techniques for calculating the central-axis depth–dose curves for irregularly shaped fields have also been developed (Hogstrom *et al* 1981, Werner *et al* 1982, Bruinvis *et al* 1983, Khan *et al* 1998).

Measurement of the central-axis depth–dose curve is therefore critical. The AAPM report of radiation therapy task group no 25 (Khan *et al* 1991) recommends a specific procedure to determine the per cent depth dose in an electron beam using a small cylindrical ionization chamber taking into account the characteristics of the chamber, the electron beam energy and its variation with depth. For energies below 10 MeV, parallel-plate chambers are recommended. If other methods of measuring the depth–dose curve are used, such as film, thermoluminescent dosimeters (TLDs) or diodes, the measurements should be compared to the data obtained with an ionization curve in water or solid phantom for a standard field size.

3.2. Absorbed dose calibration

For absorbed dose calibrations, the ionization chamber is the instrument of choice. The absorbed dose calibration of electron beams at a reference point presents special problems, because no national or international standards exist for absorbed dose to water for electron beams, except those at the National Physical Laboratory in the United Kingdom (Thwaites *et al* 2003). Although exposure standards were available when electron beams were introduced into clinical practice over 50 years ago, they applied only to lower energy photon beams. The application of the Bragg–Gray cavity theory (Gray 1936) was therefore used to determine absorbed dose for electrons. This requires determining mass collision stopping power ratios,

measuring the absorbed dose to the gas in the chamber, which requires knowing the mass of the gas, the perturbation factors and accounting for the effective point of measurement. Extensive discussions on these matters are included in ICRU Report 21 (ICRU 1972) and ICRU Report 35 (ICRU 1984) and in Klevenhagen's textbook (Klevenhagen 1993). Other dose calibration methods were also discussed, including calorimetry (Laughlin 1965, Almond 1967, Pinkerton 1969) and chemical dosimetry (Hettinger and Pettersson 1965, Shalek and Smith 1969).

The routine absorbed dose calibration for an electron beam, however, is carried out close to the dose maximum, D_m, under reference conditions (field size and treatment distance) with a calibrated ionization chamber. Because the calibration could be in terms of exposure, air kerma or absorbed dose for a stated photon beam energy, procedures had to be developed to use these calibrated ionization chambers in determining absorbed dose to water for electrons of varying energies. Svensson and Petersson (1967) and Almond (1967) were among the first investigators to look at this problem; eventually, however, national and international codes of practice or protocols were developed to accomplish this, the codes or protocols being revised or rewritten with time as different chamber calibration options became available. The international codes of practice are published by the IAEA (IAEA 1987, 1997) and the others by different national organizations (AAPM TG-21 1983, DIN 1996, IPEMB 1996, NCS 1990, NACP 1980, 1983, SEFM 1984, 1987). The references in the 1997 IAEA code of practice contain a comprehensive list of the national protocols in use at that time. Since then, the American Association of Physicists in Medicine (AAPM) protocol has been replaced (Almond *et al* 1999) and the IPEM code of practice (Thwaites *et al* 2003) has been introduced. All the protocols contain extensive references and discussions on the problems involved when using ionization chambers for the calibration of electron beams.

3.3. Dose output and monitor unit calculations

Monitor unit (MU) calculation systems require knowledge of the dose output (cGy MU^{-1}) along the central axis of regularly shaped fields at arbitrary SSD. Two popular systems for modelling output have evolved and are well discussed in the AAPM report of radiation therapy task group no 25 (Khan *et al* 1991). Both systems require measuring significant data and provide a clinical method for calculating output for arbitrary field size (defined by applicator and custom insert) and SSD. Khan (2003) reviewed the system developed at the University of Minnesota that mimicked what had been done previously for photon beams. Output at a standard SSD was determined using an equivalent square-field size (Biggs *et al* 1979). Output at an extended SSD was assumed to follow an inverse-square relationship, which required an effective SSD that was energy and field-size dependent (Khan *et al* 1978). More recently, values of SSD_{eff} as a function of energy and field size for the Clinac 2100C and 2500C were reported by Roback *et al* (1995).

Hogstrom *et al* (2000) reviewed the system developed at M D Anderson Cancer Center, which was based on the physics of electron transport. It separated the SSD dependence into an inverse-square correction based on the virtual source position (Schröder-Babo 1983), which is field-size independent, and the air gap factor, which accounts for loss of side scatter equilibrium and depends on the air gap and the field size (Meyer *et al* 1984). The method approximated irregular fields as a rectangle and used the square-root method (Hogstrom *et al* 1981) to predict the output for the rectangular field. The accuracy of the square-root method was shown to be clinically acceptable and more accurate than that of the equivalent square for the Therac 20 (Mills *et al* 1982), Clinac 2100C (Shiu *et al* 1994) and SL25 (Rashid *et al* 1990).

It is important that dose algorithms on treatment-planning systems correctly calculate dose output in water phantoms as a function of field size and SSD, so that dose calculations in the heterogeneous patient can be trusted. McNutt and Tomé (2002) developed a system that was useful for their implementation of the Hogstrom pencil-beam dose algorithm. Use of a Monte Carlo algorithm for treatment planning requires its ability to accurately calculate dose output in water, which has been studied by Zhang *et al* (1999) for the MD2 and Kapur *et al* (1998) and Verhaegan *et al* (2001b) for the Clinac 2100C. Despite their success, the potential for using Monte Carlo algorithms to calculate dose output in water for all clinical circumstances in lieu of measurement remains a worthy goal (Antolak *et al* 2002).

4. Dose measurement

The measurement of dose for electron beams can be broken down into two categories: point doses and relative dose distributions. Point doses are measured to determine dose calibration, verification of dose calibration and *in vivo* measurements to verify a patient dose. In these cases, absorbed dose measurements in Gy are required. Relative dose distributions are depth–dose curves, off-axis profiles and isodose distributions. The methods for measurement of relative dose are well established and recommendations for these methods are made in AAPM radiation therapy task group no 25 report (Khan *et al* 1991). The kind of dosimeter used, therefore, will depend on the application. In general, three types of dosimeters are used: ionization chambers, film and solid-state dosimeters.

4.1. Ionization chambers

There are a wide range of uses for ionization chambers in electron beam dosimetry. Because of their high precision and inherent accuracy, calibrated ionization chambers can be used for absolute absorbed dose calibrations, as described in section 3.2. For electron beam energies below 10 MeV, parallel-plate ion chambers are recommended to minimize perturbation and effective point of measurement considerations. Several plane-parallel ionization chambers have been designed for electron beam measurements (Morris and Owen 1975, Holt *et al* 1979, Mattsson *et al* 1981). The design criteria for plane-parallel chambers are given in IAEA Technical Report Series no 381 (IAEA 1997), and a list of available commercial chambers can be found in Klevenhagen (1993) and also in the AAPM Report no 39 (Almond *et al* 1994). At higher energies, cylindrical chambers can be used. When using ion chambers, polarity effects and perturbation effects must be taken into account. Determination of ion collection efficiency may present special consideration for electron beams. Boag (1950, 1966) developed the theory for collection efficiency in ionization chambers, and Boag and Currant (1980) modified it to a two-voltage technique, which was further developed by Weinhous and Meli (1984) and is the technique that many of the protocols recommend. Special consideration had to be given if the electron beam was swept as well as pulsed, as was the case with some linear accelerator electron beams, and Boag (1982) extended his theory to take this into account. Uncalibrated ion chambers can also be used to determine central-axis per cent depth–dose curves; however, care must be taken to apply the appropriate corrections to the reading at the different depths (Khan *et al* 1991).

4.2. Thermoluminescent dosimeters

The most frequently used solid-state dosimeters are TLDs. Because TLDs have a high sensitivity, small dosimeters can be made that are suitable for measurements in regions of

steep dose gradients frequently seen in electron beam fields and for *in vivo* dosimetry. LiF TLD is the most extensively employed TLD material with a useful dose range of 10^{-5} to 10^{1} Gy and is dose-rate independent. Although the dosimeters can be supplied in various forms (e.g., chips, rods, etc), the most common form is as a powder encapsulated in polyethylene capsules. The early use of LiF measurement of high-energy electrons was reported by Karzmark *et al* (1964) and by Suntharalingam and Cameron (1969). Although sensitivity is approximately independent of electron energy (Pinkerton *et al* 1966, Crosby *et al* 1966), it is usually recommended that TLD be calibrated in a reference radiation field at the depth-of-maximum dose on the central axis at the electron beam energy of interest. With proper care, TLD can be used for *in vivo* dosimetry and for measurements at specified points in phantoms simulating complex patient treatment, e.g., the effects of inhomogeneities that often occur as was shown in 1969 by Boone *et al* (1969) for the chest wall. However, TLDs cannot be conveniently used to measure the entire dose distribution in a phantom.

Because of readout requirements, TLD is not used for instantaneous dose-distribution determinations. However, it is ideal for mailed dosimetry where absorbed dose calibrations and depth–dose distributions need to be verified by a centralized laboratory or for intercomparisons of absorbed dose between institutions (Tailor *et al* 1999, Marre *et al* 2000).

4.3. Silicon diodes

Silicon diodes have a high sensitivity and therefore can be made very small. This allows measurements to be made with minimal perturbation to the dose distribution and to be reasonably accurate in high-dose gradient regions, e.g., regions of sharp penumbra or depth–dose fall-off. The advantage of Si diodes over TLD is that diodes have an instantaneous electronic response (Klevenhagen 1978). Si diodes can be used to measure relative dose distributions without the need for depth-dependent corrections provided their accuracy has been verified by comparison with fully corrected ionization chamber measurements of depth dose (Khan *et al* 1991). Because of these features, the p-type diode is very popular for relative electron dosimetry, for which it has been shown to be well suited (Rikner 1985). However, it is well known that its use requires consideration of directional dependence, temperature dependence and dependence on radiation damage of the sensitivity of the crystal (Rikner 1983). Marre and Marinello (2004) have evaluated these effects for commercial electron diodes used for *in vivo* dosimetry.

4.4. Film dosimetry

Film dosimetry has been used extensively as a convenient and rapid means of measuring 2D dose distributions of therapeutic electron beams. The review of film dosimetry of high-energy electrons by Dutreix and Dutreix (1969) is still applicable today and is the basis for most recommendations for film dosimetry (Khan *et al* 1991). The sensitometric curve (dose versus net optical density) must be known for the film. Ideally, this should be linear over the measured dose range, but if not, the densitometer must be able to make corrections for the shape of the curve. Film has the property of high spatial resolution and can provide a permanent record of the dose distribution. For scanned electron beams, film is often preferred to ionization chambers or diodes as the time to accumulate data can be significantly reduced.

Film dosimetry is generally used in solid phantoms, and the placement of the film in the phantom is of the utmost importance for ‘edge-on’ irradiation (Dutreix and Dutreix 1969). When the film is parallel to the beam direction, the film edge must be flush with the phantom edge. If the film protrudes or is recessed, the data on the first few centimetres of the film will

be compromised. Also, when using solid phantoms, every precaution must be taken to make sure that there are no air gaps between the film and the phantom material, which will also compromise the results. These effects have been minimized by solid water or high-impact polystyrene phantoms that are based on the Bova (1990) design, which ensures that the film is aligned with the surface. Generally, adequate compression of the phantom excludes any air pocket, particularly if bare film (removed from a light-tight packet) is used. Shiu *et al* (1989) demonstrated the excellent agreement that can be obtained between a film in a solid water phantom and an ion chamber in water for 2D dose distributions in a plane containing beam central axis.

4.5. Phantom materials

Water is recommended as the standard material for electron beam dosimetry because it is near tissue equivalent and readily available in high purity. Generally, a margin of 5 cm of phantom material beyond each side of the radiation beam and beyond the practical range of the electron beam is required. When a water phantom is not practical, such as for film dosimetry or non-waterproofed ionization chambers, a solid phantom must be used. Any solid phantom material should be as water equivalent as possible, defined as having the same linear collision stopping power and linear angular scattering power as water. This means that the electron density and effective atomic number of the phantom material must be the same as for water. Most phantoms are made from plastic, and because of their higher carbon content, true water equivalence is difficult. If the solid phantom is not water equivalent, it is necessary to correct the measured dose distribution for the effects of the phantom.

For the use of ionization chambers in solid phantoms, it is recommended that for thick-walled chambers, the phantom material should be the same as the chamber wall material, generally either polymethylmethacrylate (PMMA) or polystyrene (Khan *et al* 1991). For a thin-wall chamber, any solid phantom can be used. Care must be taken in correctly accounting for the solid material when converting to depth dose in water. High-impact, white, opaque polystyrene or electron solid water is recommended for use with film. It should be noted that, in general, for the depth dose measured in solid phantoms, the data must be corrected for effective depth and fluence in order to agree with ionization chamber measurements in water (Khan *et al* 1991).

4.6. Summary of relative dose measurements

Ten Haken *et al* (1987) demonstrated the validity of the recommendations of AAPM radiation therapy task group report no 25 for measuring relative dose by comparing electron beam central-axis depth–dose curves using film, diodes, thimble chambers and plane-parallel chambers measured in water and polystyrene against the results of measurements in water performed with a plane-parallel ionization chamber designed and optimized for use in electron beams (Mattsson *et al* 1981) at energies from 6 to 20 MeV. They found that all methods yielded reasonable results, when carefully implemented, with average differences of less than 1% or 1 mm being easily achieved (cf figure 5).

5. Electron transport calculation

Electron transport calculations have been a major factor that has allowed the quality and utilization of electron therapy to advance over the past 50 years. Before 1975, the physics of electron interactions with matter (energy loss and multiple Coulomb scatter) was mature,

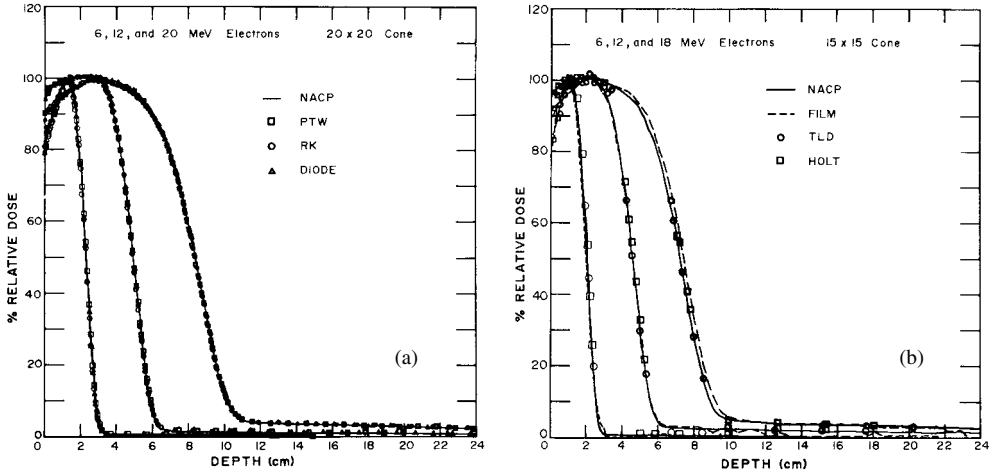

Figure 5. Demonstration of utility of concepts of AAPM radiation therapy committee report of task group 25 for electron beam dose measurements. (a) Comparison of % depth dose measured in water using the NACP parallel-plate ionization chamber, the PTW and RK 0.1 cm^3 cylindrical ionization chambers and the RFA-3 p-type diode. (b) Comparison of depth dose measured in a polystyrene phantom using Kodak XV-2 film, Harshaw LiF TLD-100 and the Holt parallel-plate ionization chamber with that measured in water using the NACP parallel-plate ionization chamber. Measurements were done at 6, 12 and 18 MeV using a Varian Clinac 1800 with the 20 × 20 cm^2 open applicator (a) and a Clinac 18 with the 15 × 15 cm^2 open applicator (b) at a nominal 100 cm SSD (from Ten Haken *et al* (1987)).

e.g., Bethe and Ashkin (1953); however, it was difficult to fully utilize that physics due to inadequate computing power and lack of applied research. The early applications of electron beam transport were reviewed in ICRU Report 21 (ICRU 1972) and by Almond (1976). This section discusses some of the important advances in transport calculations and some of their applications to date.

5.1. Analytical radiation transport

Analytical radiation transport has had the most impact on electron beam therapy to date; however, Monte Carlo calculations have made significant contributions and are becoming more influential. Analytical transport calculations have significantly impacted dose measurement, dose calculation and beam design. The doctoral dissertation of Anders Brahme (1975), much of this appearing in ICRU Report 35 (ICRU 1984), provided an eloquent formalism of how to characterize and calculate clinical electron beam parameters. Eyges (1948) scattering model, which extended Fermi's cosmic ray theory of multiple Coulomb scatter for thick targets to include energy loss, was seminal to electron beam transport, particularly its impact on clinical electron beam design and patient dose calculation. Brahme's 'geometric' characterization of electron beams (Brahme 1983) and electron transport through air (Brahme 1977) played an important role in furthering the application of Fermi–Eyges theory to beam design and patient dose calculations.

5.2. Monte Carlo transport

Electron Monte Carlo transport calculations have played an increasingly significant role in electron beam therapy. Monte Carlo calculations can provide not only a wide range of data,

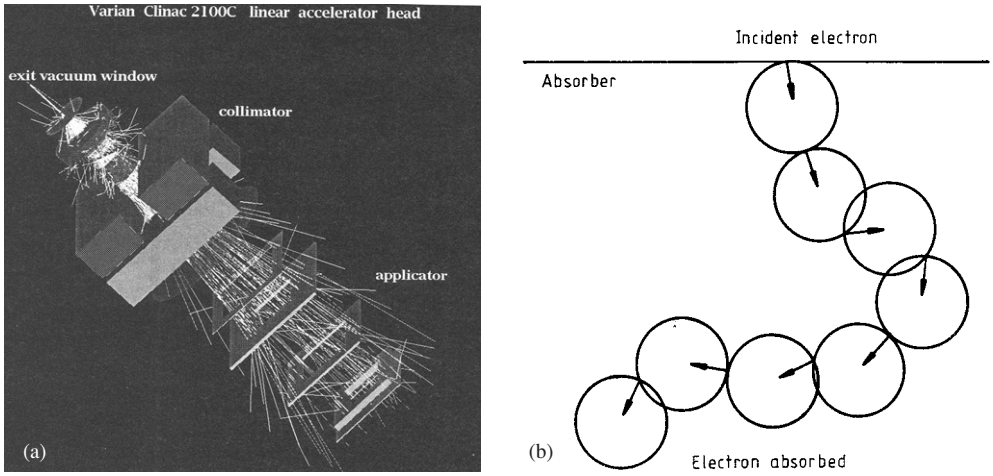

Figure 6. Overview of Monte Carlo radiation transport simulations. (a) BEAM output showing the modelling of Varian Clinac 2100C electron beam components and the resulting paths of electrons and photons transported by the Monte Carlo code (from Rogers *et al* (1995)). (b) Schematic of the macro Monte Carlo method shows how for each sphere (dependent on radius, density, material, incident electron energy) an exiting position and momentum is randomly selected using precalculated distributions, significantly speeding calculation of dose (from Neuenschwander and Born (1992)).

but often data that are difficult or impossible to measure. Early applications of Monte Carlo to electron radiation therapy utilized ETRAN by Berger and Seltzer (1969b). The impact of MC grew significantly with the availability of EGS4 (Nelson *et al* 1985), DOSXYZ and BEAM (cf figure 6(a)), the latter of which was developed as a joint effort between NRC and University of Wisconsin (Rogers *et al* 1995) and which facilitated the modelling of radiation therapy accelerators. This development was magnified further by the widespread distribution of the now EGSnrc Monte Carlo code through an annual course on BEAM (http://www.irs.inms.nrc.ca/irs.html). Also, Ma *et al* (2002) have made available MCDOSE, a Monte Carlo code adapted to perform patient planning using computed tomography (CT) data (http://www.fccc.edu/cancer/treatment/radonc/treatment/monte-carlo-course.html). Results of MCNP (Brown *et al* 2002), which has played a lesser role in electron beam therapy, were compared with those of EGS4 by Jeraj *et al* (1999) for clinical electron beams, and van der Zee *et al* (2005) compared results from MCNP-based ORANGE with those of DOSXYZ. MCNP is also available through ongoing courses (http://laws.lanl.gov/x5/MCNP/classinformation.html).

5.3. Applications of radiation transport

5.3.1. Dual-scattering foil and TSEI beam design. Narrow electron beams exiting linear accelerators and directed towards the patient using a bending magnet are made broad and flat typically using a dual-scattering foil system. Kainz *et al* (2005) demonstrated the utility of the analytical scattering formalism of Green (1991) for designing dual-scattering foil systems and how the results agreed with EGS4 Monte Carlo transport. Antolak and Hogstrom (1998) demonstrated how the analytical formalism of Huizenga and Storchi (1987) can be used to design beams for total-skin electron irradiation and to predict their off-axis fluence distribution. Ye *et al* (2005) showed similar utility using EGS4 Monte Carlo.

5.3.2. Electron collimation. Analytical theory can be readily used to design the required lateral dimensions of the multiple collimating levels used in electron beams. This was demonstrated for design of intraoperative cones (Hogstrom *et al* 1990), a variable trimmer collimator (Hogstrom *et al* 1985) and an electron multi-leaf collimator (Hogstrom *et al* 2004). However, in some instances it is necessary for the collimator design to include effects of collimator leakage and scatter, which requires using Monte Carlo transport. Such effects have been studied for existing electron applicators from major suppliers (van Battum *et al* 2003) and for various attributes of electron multi-leaf collimators (eMLC) (Lee *et al* 2000). Karlsson *et al* (1999) used BEAM Monte Carlo in a study of the use of helium in the treatment head for eMLC design.

5.3.3. Beam dosimetry. Electron dosimetry calculations often require knowledge of beam energy at depth, which was determined by the Harder (1965) relationship, $E_z = E_0(1-z/R_p)$. ICRU Report 35 (ICRU 1984) recommended relationship between incident electron beam energy, E_0, and the practical range, R_p, was based on ETRAN calculations of Berger and Seltzer (1969a). The conversion of measured ionization to dose requires the ratio of the mass stopping power of water to air as a function of depth and initial beam energy, which were determined by Berger using ETRAN and are found in ICRU Report 35 (ICRU 1984). Subsequently, more accurate values for clinically realistic beams, determined using BEAM by Ding *et al* (1995), serve as the basis for conversion of ionization to dose in the most recent AAPM dose calibration protocol (Almond *et al* 1999). Reports of AAPM radiation therapy committee task groups 21 (AAPM 1983) and 25 (Khan *et al* 1991) recommended how to transfer measurements of calibration dose and depth dose in plastic to that in water. The depth-scaling factors were based on measured values of R_{50}, and the fluence correction factors were based on analytical dose calculations using Eyges scattering theory for monoenergetic, parallel beams (Hogstrom and Almond 1982). Monte Carlo calculations should improve the accuracy of converting measurements made in plastic phantoms by providing more accurate values using BEAM for depth-scaling factors (Ding and Rogers 1996) and fluence correction factors (Ding *et al* 1997) and PENELOPE for fluence correction factors (Siegbahn *et al* 2003).

6. Treatment planning

6.1. Evolution of dose algorithms for treatment planning

By the 1970s, electron beams were becoming more readily available, and clinical demand to accurately compute dose in the presence of tissue heterogeneities became a major concern. At that point in time, the status of electron beam dose calculations and treatment planning was reviewed by the AAPM (1978) and Nüsslin (1979). Up until that point, algorithms available to clinical medical physicists for calculating dose were based largely on measured dose distributions in water. The matrix method of Milan and Bentley (1974), developed primarily for photon dose calculations, had been implemented into the commercially available RAD-8 treatment-planning system and later the General Electric RT/Plan and was being used for electron beam dose calculations, despite its inaccuracy due to its lack of appropriate modelling of the physics. Another methodology based on measured data was that being used by the Memorial Sloan-Kettering Cancer Center (Mohan *et al* 1981). In both of these systems, corrections for patient heterogeneity were 1D, i.e., assumed slab homogeneities, which did not account for the significant impact of lateral multiple Coulomb scattering on the dose distribution. Also, corrections for variation of SSD were based on interpolating measured data or simply modelling beam divergence.

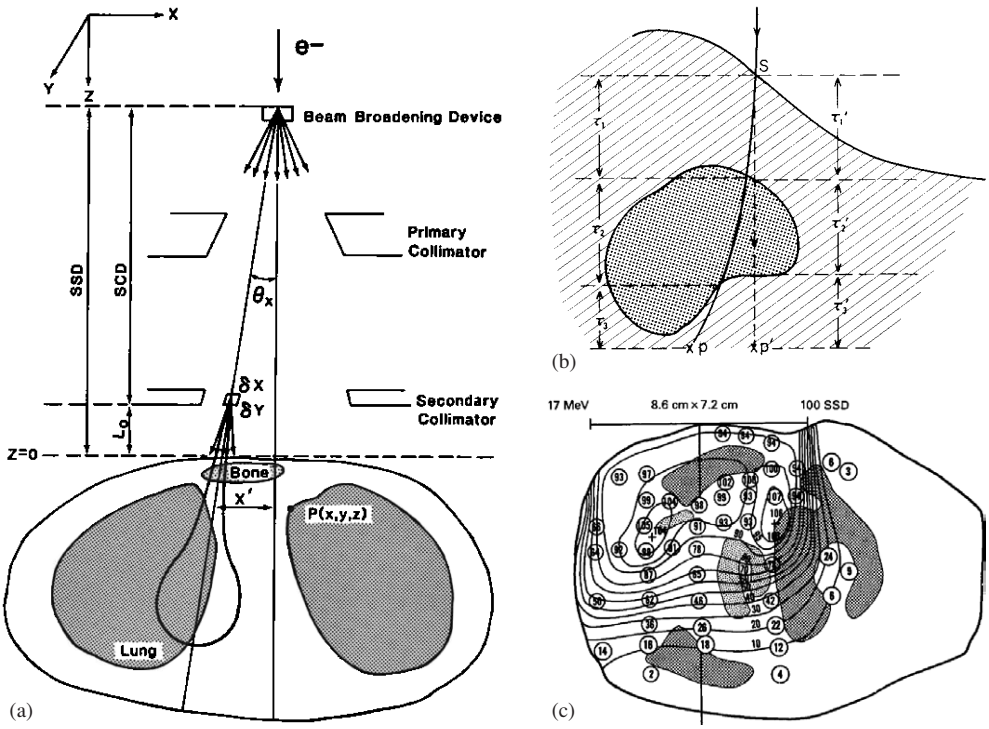

Figure 7. (a) Schematic view of the Hogstrom PBA showing that it was modelling beam collimation, air gap (L_0) and internal patient heterogeneity (from Hogstrom *et al* (1981)). (b) PBAs were restricted to using the central-axis approximation for the pencil beam's anatomy, first illustrated by Perry and Holt (from Perry and Holt (1980)). (c) Early verification of the Hogstrom PBA in patients was assessed by TLD measurements in 2D cylindrical phantoms designed from a transverse patient CT scan (from Hogstrom *et al* (1984b)).

Lillicrap *et al* (1975) showed that the measured broad-beam dose distributions in water could be predicted by summing the measured dose distribution from many smaller beams, referred to as pencil beams. Kawachi (1975) showed that the dose distribution in water could be calculated using a model based on diffusion theory, and Steben *et al* (1979) and Mandour *et al* (1983) contributed minor improvements to the parameterization, further validation and the concept of summing pencil-beam dose distributions calculated using diffusion theory. To account for internal heterogeneities, investigators realized that pencil beams could only work if there were improved methods for calculating these distributions in the presence of tissue heterogeneities.

Simultaneously and independently, several investigators turned to the Fermi–Eyges theory of thick target multiple Coulomb scattering (Eyges 1948) for the solution. Perry and Holt (1980) first demonstrated how the mean path length of an electron pencil beam can be approximated by the central pencil-beam axis, accurately predicting dose distributions beneath an irregular surface (cf figure 7(b)). The pencil-beam algorithm (PBA) by Hogstrom *et al* (1981), who first used the Fermi–Eyges pencil-beam theory to calculate dose in patients (cf figure 7(a)), was unique in that it showed how to (1) input measured square-field central-axis depth dose in water data to accurately calculate dose for any field size, (2) utilize CT data on a pixel-by-pixel basis, (3) accurately model variable air gap, and (4) redefine pencil beams at the surface, accurately calculating the effect of irregular surface on dose homogeneity,

regardless of the air gap. The Hogstrom version of the PBA was successfully implemented into the General Electric RT/Plan treatment-planning system, and Hogstrom *et al* (1984b) demonstrated its accuracy for a number of clinical simulations (cf figure 7(c)). Due to computer limitations in memory and speed of calculation, early implementations of the PBA were multi-planar; however, as computing technology advanced, Starkschall *et al* (1991) showed how to implement the Hogstrom PBA in 3D. That implementation presently serves as the basis for electron dose calculations for many commercial 3D systems, e.g., Pinnacle and FOCUS.

Fermi–Eyges theory underestimated large angle scattering and hence the pencil-beam width. This effect was offset by another shortcoming: the assumption that all electrons reached the depth of the practical range, which was not true as electrons scattered through a larger angle have a shorter range. Werner *et al* (1982) addressed the latter, showing that the calculation of the sigma of the pencil-beam Gaussian lateral distribution be improved by modifying the value for the final third of the practical range. Lax *et al* (1983) addressed the former, showing how a 3-Gaussian kernel for the scatter distribution improved the accuracy of the calculation. This enhanced their PBA (Brahme 1981), which was also implemented into some commercial treatment-planning systems, e.g. Varian's CADPLAN.

Accuracy and possible limitations of the PBA or any algorithm must be demonstrated, and this required a reasonable measured data set of dose distributions for controlled geometries that mimic actual patient tissues and geometries. The NCI-funded Electron Collaborative Working Group produced such a data set (Shiu *et al* 1992), which has been publicly available through M D Anderson, as has been a more recent data set by Boyd *et al* (2001a). The former was useful in evaluating early 3D versions of the pencil-beam algorithms (McShan *et al* 1994, Cheng *et al* 1996) and the voxel Monte Carlo (Fippel *et al* 1997), and the latter has been useful for the evaluation of the PBRA (Boyd *et al* 2001b) and the macro Monte Carlo algorithm (Popple *et al* 2005). Similar data were used to test the Lax and Brahme PBA in CADPLAN (Samuelsson *et al* 1998), the Hogstrom PBA in FOCUS (Muller-Runkel and Cho 1997) and a result based on both PBAs in Helax-TMS (Blomquist *et al* 1996).

Brahme (1985) and Hogstrom and Steadham (1996) reviewed the status of pencil-beam dose algorithms, showing the limitations of the PBA, which was primarily due to the central-axis approximation. Initially, this limitation led to improved analytical dose algorithms such as the phase space evolution algorithm (Huizenga and Storchi 1989, Janssen *et al* 1994, Korevaar *et al* 1996), the pencil-beam redefinition algorithm (PBRA) (Shiu and Hogstrom 1991, Boyd *et al* 1998, 2001b) and an extension Jette's original PBA theory (Jette and Walker 1992), reviewed by Jette (1995). Although these analytical algorithms can accurately calculate dose in patients, there has been a more recent trend towards Monte Carlo dose algorithms based on EGS4. Monte Carlo algorithms are computing intensive, and the idea to use precalculated kernels in a macro Monte Carlo by Mackie and Battista (1984) has led to the development of Monte Carlo dose calculations for treatment planning. Neuenschwander and Born (1992) and Neuenschwander *et al* (1995) developed the macro Monte Carlo method for electron beam dose calculations (cf figure 6(b)). Keall and Hoban (1996) developed the super Monte Carlo dose algorithm that similarly pregenerated electron track kernels. Kawrakow *et al* (1996) developed the voxel Monte Carlo (VMC), which was successfully implemented into a commercial treatment-planning system (MDS Nordion, Ottawa, ON, Canada) and evaluated by Cygler *et al* (2004). Monte Carlo dose algorithms will likely play a significant role in future electron beam planning, and their use in the clinic will likely increase as their commissioning becomes easier and more accurate. Numerous investigators have reported on differing levels of success in modelling electron beams using Monte Carlo to predict electron beam dose distributions, and the difficulty is best summarized by Antolak *et al* (2002) who challenged

the medical physics community to demonstrate 2% or 0.1 cm agreement between measured and calculated doses over the entire range of clinical treatment parameters. Such difficulties in beam commissioning have stimulated analytical source modelling such as the multi-source modelling by Ma *et al* (1999).

Despite the significant progress in calculating dose, treatment-planning systems currently fail the practice of radiation therapy and the treatment of patients with electron beam therapy by being unable to model actual treatments. Treatment-planning tools, such as skin collimation, internal collimation and bolus, are modelled inadequately or not at all.

6.2. CT in electron beam treatment planning

The use of CT scanners in radiation therapy has transformed the methods by which radiation therapy treatment planning is done. Today, CT simulators have essentially replaced x-ray simulator technology. CT scanners began emerging in many treatment-planning centres around 1980, and their utility was introduced in conferences soon after (Ling *et al* 1983, AAPM 1983). CT scans were important for diagnosis, staging and subsequently specifying the 3D planning target volume (PTV). Hogstrom (1983a) reviewed the early implementation of the CT scanner in the radiation therapy paradigm.

CT scan data provide a 3D model of the patient, which is necessary for planning and visualizing the dose distribution. This function is important for planning electron beams, because prior to CT, it was not possible to precisely view how an electron beam can treat a superficial PTV and its dose distribution stopping short of over-irradiating distal critical structures (Hogstrom and Fields 1983). Equally significant, CT provided the patient data necessary for the calculation of dose. The PBAs required knowledge of electron stopping and scattering powers, which could be correlated to CT number (Hogstrom *et al* 1981), and Monte Carlo algorithms required knowledge of tissue type and density, which can also be correlated to CT number (Schneider *et al* 2000).

6.3. Electron treatment-planning basics

There are several physical characteristics of the electron beams and fundamental principles that must be considered when planning patient treatment with electron beams (Hogstrom 2004):

- *Sharp dose fall-off and energy selection.* A unique property of electron beams is that their sharp fall-off in depth dose beyond R_{80} (depth of 80% of maximum dose on distal fall-off) offers protection for the anatomical structures beyond the PTV. This allows superficial PTVs to be treated with a single en-face beam, something not possible with photon beams. The maximum depth of the PTV determines the beam energy; in unit density tissue, the electron energy should be at least approximately 3.0 (3.3) times the maximum depth of the PTV in cm to cover the PTV with the 80% (90%) relative dose.
- *Dose build-up.* Within a few centimetres of tissue, the dose approaches 90% of the dose at the depth of dose maximum resulting in modest skin sparing. The relative surface dose is lowest for the low-energy electron beams ($\approx$70% at 6 MeV) and greatest for the high-energy electron beams ($\approx$95% at 20 MeV), which is the reverse of photon beams. If low-energy electron beams are being used and a high skin dose is required, then bolus is often used to increase the skin dose, requiring the optimal energy–bolus combination.
- *Constrictions of the isodose curve at depth.* There is considerable constricting of the 80–90% isodose curves as the depth increases to R_{90} (Hogstrom 1991). For the example of 15 MeV beam in figure 1(a), a constriction of approximately 0.75 cm is seen at the depth of $0.5 \times R_{90}$. This means, for example, that a surface field defined as a 6 cm

circle at the surface will have an effective diameter of 4.5 cm across the 90% isodose curve, and this must be taken into account in treatment planning.

- *Normal incidence*. Electron beams are usually most effective when they are incident perpendicular to the surface. Ekstrand and Dixon (1982) and Biggs (1984) showed the negative impact of non-perpendicular incidence on the depth dose in the patient.
- *Dose perturbations due to tissue heterogeneity*. Due to the dependence of electron beam scattering and the range of the electrons upon density and atomic composition, the effects of tissue heterogeneity upon the dose distribution are more pronounced for electron beams than for photons. The effects of irregular patient surface, bone, lung and internal air cavities on the dose distribution can be significant, causing dose heterogeneity in the PTV, geographical miss of the PTV in depth and increased dose to normal tissues and critical structures. The impact of tissue heterogeneities on patient dose distributions, the subject of many early investigations into electron beam dose distributions, has been reviewed by Hogstrom (1983b, 2004), ICRU Report 35 (ICRU 1984) and AAPM radiation therapy committee task group no 25 (Khan *et al* 1991).
- *Beam mixing*. Tapley (1976) showed how the mixing of one fraction of megavoltage x-ray beam, e.g. 18 MV, with three to four fractions of electron beams allowed the planner to custom design the central-axis dose distribution. This function was particularly useful in patients for whom skin sparing was required, i.e., lower entrance dose, or for penetration slightly deeper than the therapeutic range for the highest energy electron beam. This was easily accomplished using optimization software (Fields and Hogstrom 1982, 1984, Starkschall *et al* 1990). Also, the possibility of mixing electron beams allows the treatment planner to increase surface dose by adding low-energy beams or a low-energy bolused beam (Hogstrom 1991, 2004). Leavitt *et al* (1990b) showed that this could be particularly useful for arc electron therapy.

6.4. Treatment and treatment-planning tools

Electron beam treatments can be greatly enhanced by utilization of tools that help achieve the treatment objective. The most standard tool is the irregularly shaped treatment field, which is formed using Cerrobend inserts placed inside electron applicators, a technology early demonstrated by Goede *et al* (1977) and modelled in current treatment-planning systems. Hogstrom (2004) recently reviewed the fundamentals for utilizing additional tools, such as skin collimation, internal collimation, bolus and abutment techniques.

Skin collimation has played an important role in electron therapy by creating the sharpest possible penumbra to protect adjacent critical structures. Skin collimation is used frequently for skin cancers (Tapley 1976), chest-wall arc therapy (Leavitt *et al* 1990a) and decreasing penumbra enlarged by extended SSD or bolus scatter plates above the irregular patient surface (Hogstrom 1991). Despite the utility of skin collimation and its frequent use in the clinic, treatment-planning systems have failed to provide adequate tools for modelling skin collimation and calculating dose in its presence, although there can be a 'workaround' in some instances (Hogstrom and Steadham 1996). Verhaegan *et al* (2001a) and Chi *et al* (2005) demonstrated the utility of Monte Carlo and the PBRA, respectively, for calculating dose in the presence of lead skin collimation.

Internal collimation is useful in that it can protect critical structures directly in the treatment field, e.g., salivary glands using intraoral stents (Tapley 1976). Also, eye shields are used to protect the lens and cornea, particularly in treatment of skin cancer near the eye. Shiu *et al* (1996) developed electron-specific eye shields made of tungsten while demonstrating that x-ray eye shields made of lead have inadequate thickness to stop 6 MeV electrons. Of

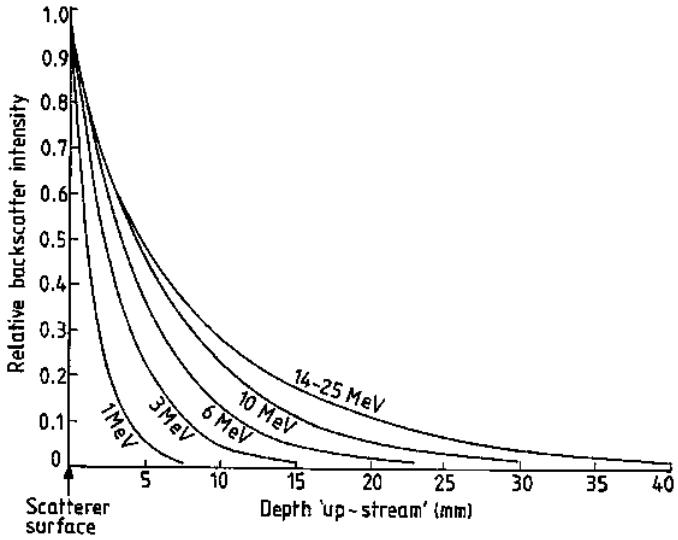

Figure 8. Plot of relative ionization due to backscatter versus depth upstream in polystyrene resulting from a broad electron beam incident on lead. Each curve represents results for the energy of the beam incident on the polystyrene–lead interface (from Lambert and Klevenhagen (1982)). Magnitude of backscatter ionization is given by Klevenhagen *et al* (1982).

particular significance is knowing the amount of backscatter dose from internal collimation to prevent complications to upstream tissues. Klevenhagen *et al* (1982) reported the magnitude of backscatter from lead collimation, and Lambert and Klevenhagen (1982) reported its penetration upstream (cf figure 8). These data allow determination of wax or other low-Z material that can be placed on the lead or tungsten to protect upstream tissue.

Hogstrom (1991, 2004) defined electron bolus as water or near-water-equivalent material that is normally placed either in direct contact with the patient's skin surface, close to the patient's skin surface, or inside a body cavity and that provides extra scattering or energy degradation of the electron beam. Constant-thickness bolus is used both to increase dose to the patient's skin surface and to fine tune depth of penetration so that there is an optimal energy–bolus thickness combination (Hogstrom 1991). Bolus also serves as a missing-tissue compensator for surface irregularities and internal air cavities, particularly for the ear canal (Morrison *et al* 1995) and the nasal passageway (Hogstrom 2004). Variable-thickness bolus, used to achieve conformal electron therapy, is discussed later.

7. Clinical use of electron therapy

The characteristics of the electron beam that make it a unique therapeutic modality are related to its physical qualities. The mechanisms for energy deposition and clinical radiobiology are the same for electrons as for photons, so the treatment aims and therapeutic principles are similar to those that have been established for megavoltage photon beam treatments. Treatment techniques are only modified from photon treatments to accommodate the specific dose distribution characteristics of the electron beams. These characteristics give it a distinct advantage in treating malignant lesions located at a limited depth. A sterilization dose can be delivered to the tumour while the total volume of irradiated tissue is sharply limited. Electron

beam therapy is a modality complementary to x-ray therapy, which allows treatment of cancer within 6 cm of the surface.

Electron beam energies in the range of 6–20 MeV are principally used in the treatment of (1) skin and lip cancers, (2) chest-wall and neck (elective post-surgery and recurrent disease) cancers, (3) upper respiratory and digestive-tract lesions from 1 to 5 cm in depth (using the electron beam alone, in combination with photon beams, in association with interstitial therapy or as a boost treatment to primary lesions), and (4) boost treatment to lymph nodes, operative scars and residual tumour. The clinical utilization of the electron beam using the treatment and treatment-planning tools discussed above was described in the first comprehensive textbook on electron radiation therapy by Norah duV Tapley at M D Anderson (Tapley 1976) and subsequently by Meyer and Vaeth (1991).

Medical physicists have contributed significantly to special procedures using electron beams. Special procedures are defined as procedures that are infrequently encountered in a typical radiation therapy clinic and for which the utilization of electron beam therapy requires special beams, collimating devices, planning procedures and treatment devices. Such procedures are often offered in regional cancer centres where sufficient numbers of patients allow for sufficient expertise and economy.

7.1. Total-skin electron irradiation

Total-skin electron irradiation (TSEI) is utilization of low-energy electron beams to treat the total skin of the patient. Typically, this technique is used for treatment of cutaneous T-cell lymphoma, which is usually referred to as mycosis fungoides. Mycosis fungoides is rare, having an incidence rate of 3 in 10^6 people in the age group of 45–69 years (Greene *et al* 1979). The technique was used as early as 1952 by Trump in Boston, using a 2.5 MeV Van de Graaff generator (Trump *et al* 1953). The technique made a significant step forward in 1957, when Stanford began its utilization of a six-field technique (Karzmark *et al* 1960). Memorial Sloan-Kettering later offered a four-field technique (Edelstein *et al* 1973) that utilized a scatter plate directly in front of the patient, making the patient dose distribution comparable to that of the Stanford technique (Holt and Perry 1982). In TSEI, the lateral dimension (90–90% width) of the electron beam should be at least 60 cm at the patient treatment plane, and it is elongated in the inferior–superior dimension by using two gantry angles (Stanford technique) or three gantry angles (Memorial Sloan-Kettering technique). In the mid 1980s, M D Anderson Cancer Center commissioned the Stanford six-field technique, adding the concept of the Memorial Sloan-Kettering scatter plate (Hogstrom *et al* 1984a, Almond 1987), now the standard technique used in many institutions. Methods of dose calibration, relative dose measurements, calculation of MU and quality assurance are all unique to this technique, and these methods along with other practical information were published in AAPM Report no 23 (AAPM 1987).

Despite the best efforts to achieve uniform dose, methods for shielding and boosting various parts of the body are required. Techniques for this have evolved from the early providers of TSEI and are described in AAPM Report no 23. The need for shielding and boosting is based on *in vivo* TLD. Results using the original Stanford technique were reported by Palos and Fessenden (1982) at Stanford and Fraass *et al* (1983) at the National Cancer Institute; results for the Stanford technique with an acrylic scatter plate in front of the patient were reported by Desai *et al* (1988) at City of Hope National Medical Center, Weaver *et al* (1995) at the University of Minnesota and Antolak *et al* (1998) at the M D Anderson Cancer Center.

Despite (1) the evolution of the technique into the relatively popular modified Stanford technique, (2) the development of reasonable dosimetry recommendations by AAPM Report

no 23, and (3) the benefit of the technique to mycosis fungoides patients, e.g. Hoppe (2003), Duvic *et al* (1996, 2003) and Ysebaert *et al* (2004), manufacturers have been slow to fully support this technique. Most accelerator manufacturers offer a high dose rate option for TSEI; however, they do not offer the patient stand and scatter plate, the external scattering foil, methods for calibration and QA of the technique, and interlocks for all beam, collimation and gantry settings.

7.2. Total-limb irradiation

A variation of the TSEI technique is total-limb irradiation. This technique uses six to eight broad beams at conventional SSDs (100–110 cm) to irradiate superficial disease of the limb (arm or leg), e.g., melanoma, lymphoma, Kaposi's sarcoma and myeloma. Wooden *et al* (1996) demonstrated how to use this technique for irradiating Kaposi's sarcoma of the lower calf, and Hogstrom (2004) reviewed the technique for other sites.

7.3. Intraoperative electron therapy

Intraoperative radiation therapy (IORT) delivers a single radiation fraction to the surgical bed to treat unresected tumour, tumour remaining from partial resection or adjacent tissues containing microscopic tumour cells. Clinical uses of IORT were summarized in conference proceedings by Meyer and Vaeth (1991) and Meyer and Hinkelbein (1997). According to Jones (1991), IORT using x-ray beams was described as early as 1909 (Beck 1909), and IORT with electrons using a betatron was reported by Abe and Takahashi (1981).

Intraoperative electron therapy (IOET) is unique in that (1) it is delivered in a single fraction, (2) electron cones designed specifically for IOET are used, (3) the electron cone should not be in physical contact with the accelerator (to prevent injury to patient from collision with the cone), and (4) it must be delivered in a sterile environment, i.e., the operating room must become a radiation treatment room or vice versa.

Early cone design, described by Biggs *et al* (1981), McCullough and Anderson (1982), Fraass *et al* (1985) and Hogstrom *et al* (1990), discussed principles of cone size (diameter and length), shape (circular, rectangular and squircle), angled end (0–30°) and radiation leakage (scattered around or through the cone wall). The electron cone, once accurately placed and immobilized in the patient, must be aligned with the treatment machine, a process called docking. Hard docking places patients at risk for injury, so soft-docking systems are typically used. Soft-docking systems, reviewed by Palta *et al* (1995), utilize laser or other optical systems to allow accurate alignment while maintaining an air gap of several centimetres between the two.

Retrofitting the radiation therapy linac room for IOET requires that the treatment machine be unavailable for service during the time the room is prepared for the sterile patient, waiting time and time to restore the room for conventional treatment. Therefore, in the early 1980s, there was a push to make dedicated electron accelerators for the operating room. Rich (1986) was a strong proponent of IORT, and he led a collaborative effort between M D Anderson and Siemens Medical Systems to develop the Siemens dedicated IOET linac with electron energies of 6–14 MeV (Rich and Dally 1985). This utilized solutions to operating room shielding (Mills *et al* 1990) and cone design (Hogstrom *et al* 1990). One beneficial feature was the use of an operating room couch in lieu of the standard radiation therapy linac couch (Fraass *et al* 1985). With the Siemens unit no longer available, a compact electron radiation therapy machine that could be wheeled between operating rooms, the Mobetron (energies from 4–12 MeV), became a product. Presently, it is the only known commercially available option (Meurk *et al* 1997, Mills *et al* 2001).

The dosimetry and treatment planning for IOET is simple in that it is not possible to construct 3D CT-based treatment plans. Rather, treatment planning consists of comparing the physician's evaluation of the target volume with selecting the best cone and energy based on isodose curves in water. These and output data needed to determine the number of monitor units to deliver the prescribed dose were demonstrated by Nyerick *et al* (1991). IORT fundamental techniques, dosimetry, dose specifications and recommendations for the clinical medical physicist were published in an AAPM radiation therapy task group report (Palta *et al* 1995).

7.4. Total-scalp irradiation

Electron beams can deliver total-scalp irradiation used to treat melanoma, lymphoma and angiosarcoma of the scalp. Historically, Tapley (1976) utilized a set of patched fields to treat the hemispherical surface of the scalp. Able *et al* (1991) showed the highly tedious technique to be marginally acceptable from a dosimetric point of view, even moving the field borders to feather the regions of dose overlap and hot spots. Akazawa (1989) provided a more practical solution to this treatment by abutting lateral electron beams that treated the lateral scalp with parallel opposed x-ray beams used to irradiate the rind of the scalp. Tung *et al* (1993) subsequently improved the dose distribution of that technique by modifying the abutment scheme to incorporate the effect of beam divergence.

7.5. Craniospinal irradiation

Another frequent use of abutting electron and x-ray beams is craniospinal irradiation, used to treat paediatric tumours of the brain, base of brain and spinal theca, e.g., medulloblastoma, malignant ependymoma, germinaoma and infratenorial glioblastoma. This technique used parallel opposed lateral x-ray beams to treat the brain and base of brain, which abut a posterior electron field used to irradiate the spinal cord. The absence of exit dose to the patient's anterior reduces the probability for many acute and late effects, which are of particular importance to paediatric patients. This technique, used in lieu of photon fields to irradiate the spinal cord theca, was simultaneously developed at M D Anderson Cancer Center by Maor *et al* (1985) and the University Hospital in Leuven by Dewit *et al* (1984).

7.6. Electron arc therapy

The primary use of electron arc therapy has been for chest-wall irradiation, particularly in cases of bilateral disease, a barrel-chest anatomy and posterior extension. Its clinical utilization has been best studied by the University of Utah group (Peacock *et al* 1984, McNeely *et al* 1988, Stewart *et al* 1991). Their treatment technique is highly refined and well described by Hogstrom and Leavitt (1987).

Dosimetry for arc electron therapy has some unique characteristics due to the fact that there is a large air gap between the secondary collimator and the patient and the converging fluence in the plane of rotation. Khan *et al* (1977) and Ruegsegger *et al* (1979) reported on these properties, whose physical basis was reviewed by Hogstrom and Leavitt (1987). These and the use of a shaped secondary collimator and skin collimation (Leavitt *et al* 1990) place special needs on dose algorithms beyond those used for fixed electron beams. Early dose algorithms were based on either interpolated measured data (Leavitt *et al* 1985, Lam *et al* 1987) or parameterization, e.g., the angle-beta concept (Pla *et al* 1989, 1991, Olivares-Pla *et al* 1997). Hogstrom *et al* (1989) adapted the PBA to an arc beam geometry, implementing it for multi-planar dose calculations. Kurup *et al* (1992) and Antolak *et al* (1993) evaluated the accuracy of

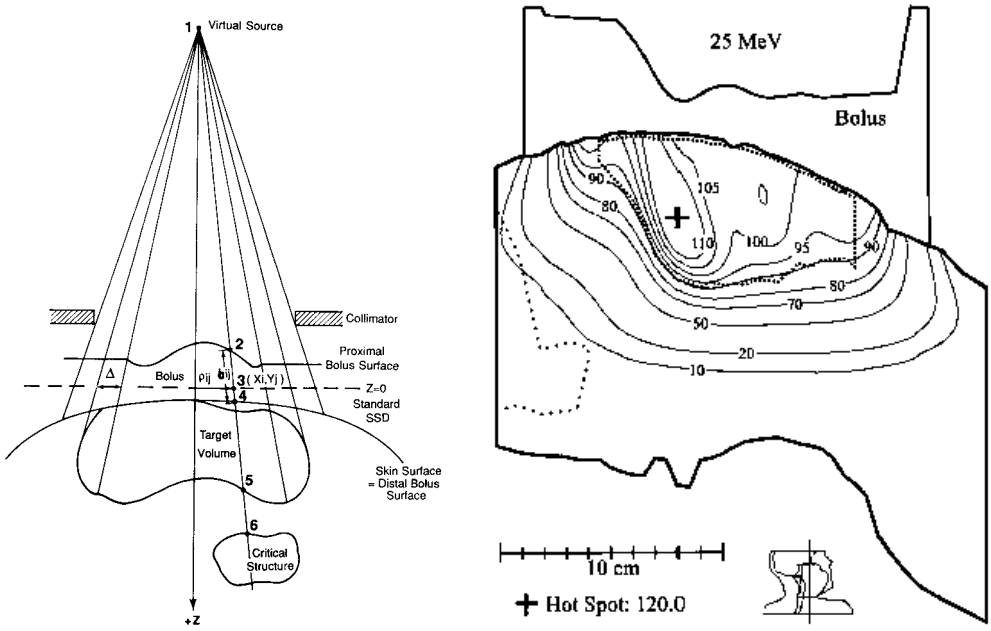

Figure 9. (a) Schematic of bolus design algorithm accounting for range shifting and multiple scattering (from Low *et al* (1992)). (b) Dose distribution in the coronal plane for a patient having squamous cell carcinoma of the right buccal mucosa planned in the 'open neck' position using bolus conformal therapy with a 25 MeV beam. The 'hot spot' is due to the sharp bolus gradient and could be eliminated using intensity modulation (from Kudchadker *et al* (2002)).

the algorithm, which predicted the geometrical effects of arced beams well, but suffered from the same inaccuracies as did the fixed-beam PBAs due to the central-axis approximation. That algorithm was clinically useful and commercially available for several years on the General Electric Target treatment-planning system, which is no longer manufactured. More recently, Chi (2004) and Chi *et al* (2006) addressed the inaccuracy issue by summing dose distributions calculated using the PBRA. Presently, no manufacturer is known to offer a treatment-planning system that models electron arc therapy.

7.7. Electron conformal therapy

Hogstrom *et al* (2003) defined electron conformal therapy (ECT) as 'the use of one or more electron beams for the following purposes: (1) containing the PTV in the 90% (of given dose) dose surface, (2) achieving as homogeneous a dose as possible (e.g., 90–100%) or a prescribed heterogeneous dose distribution to the PTV, and (3) delivering a minimal dose to underlying critical structures and normal tissue.' To date, patient treatment has been restricted to two types of ECT: bolus ECT and segmented-field ECT. Bolus ECT is similar to the technology that evolved for heavy-particle beams (i.e., pions, protons and heavy ions). Early bolus utilization by Beach *et al* (1981) and Archambeau *et al* (1981) was inaccurate due to unavailability of adequate dose calculation algorithms and a design that neglected multiple Coulomb scattering. Low *et al* (1992) first showed how to design electron bolus by accounting simultaneously for both range shifting and multiple Coulomb scattering (cf figure 9(a)). The bolus, shaped on one side to fit the patient's surface anatomy and on the other side to conform the 90% dose

surface to the distal surface of the PTV, was milled from machineable wax by an automatic milling machine. This technique's utility was demonstrated for the chest wall (Perkins *et al* 2001), head and neck (Kudchadker *et al* 2002, 2003) (cf figure 9(b)) and paraspinal muscles (Low *et al* 1995). Kudchadker *et al* (2002) showed how the addition of intensity modulation improved the homogeneity of PTV dose; however, this enhancement requires the use of an eMLC, technology not yet available. Bolus ECT technology is expected to be commercially available soon.

Segmented-field ECT is 'the utilization of multiple abutted electron fields, each having a common virtual source position but each having its own energy and weight, so as to conform the therapeutic dose surface (e.g., 90% of given dose) to the PTV.' (Hogstrom *et al* 2003). This technique can be done using multiple fields defined by Cerrobend cutouts or by a suitable MLC (Zackrisson and Karlsson 1996). Presently, treatment planning is done by trial and error as manufacturers do not have algorithms for optimizing the segmentation and weighting of the multiple beams of differing energies. Hogstrom *et al* (2003) have discussed the pros and cons of the bolus and segmented-field ECT techniques. Another ECT technique, utilizing energy and intensity modulation, has not been used on patients, but offers significant promise in the future and is discussed below.

8. Future of electron therapy

Electron therapy has served and will continue to serve radiation oncologists well in the management of superficial disease. Particularly important to its future are the commercial availability of proper technology and the proper training of radiation oncologists and allied professionals. Additionally, as radiation therapy technology changes, undoubtedly the role of electron beam therapy will also.

8.1. Future challenges to electron therapy

Presently, treatment-planning systems cannot properly model electron therapy (e.g., skin collimation, internal collimation, variable-thickness bolus and arc therapy) and thus cannot take full advantage of existing treatment technology. Also, treatment machines lack sufficiently fine energy spacing (e.g., 1 MeV) to provide optimal therapy. This technology will not become available so long as the radiation therapy community does not require it from the manufacturers, and this is not likely to happen unless the education of radiation oncologists in electron therapy improves. That process will remain impaired unless radiation oncologists have access to proper technology. This creates an unfortunate circular dilemma.

The problem of underutilization of electron therapy is exacerbated by new technology. The TomoTherapy HI·ART machine (TomoTherapy Inc., Madison, WI) offers serial IMXT and has no electron beam capability, so TomoTherapy users are investigating those superficial treatment volumes that can be treated using tomotherapy in lieu of electron beam therapy, e.g. total scalp (Orton *et al* 2005, Locke *et al* 2002), craniospinal (Peñagarícano *et al* 2005) and chest wall. Also, as intensity-modulated radiation therapy (IMRT) allows the user to avoid normal tissues in the head and neck (Lee *et al* 2005), e.g., spinal cord and salivary glands, the use of electrons will decrease.

Proton therapy has similar properties as electron therapy, but has sharper dose fall-off due to its greater mass, greatly reducing the magnitude of lateral multiple Coulomb scatter. Undoubtedly, most electron treatments could be better delivered with a proton beam; however, the cost of proton therapy is at least an order of magnitude greater. Investigators have shown its dose distributions to be superior to those for x-ray therapy for treatment of medulloblastoma

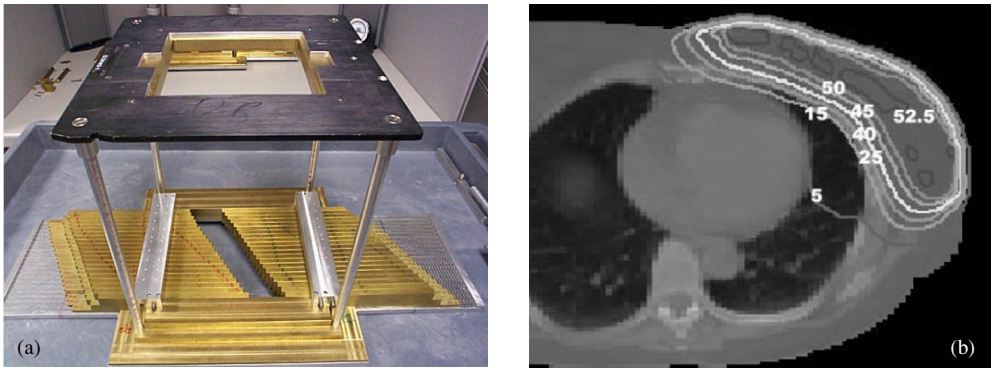

Figure 10. (a) View of prototype electron multi-leaf collimator (from Hogstrom *et al* (2004)). (b) Intact breast treatment plan using eight-field modulated electron radiation therapy, which spares normal tissue better than standard x-ray and IMXT treatment plans. Isodoses are in units of Gy (redrawn from Ma *et al* (2003)).

(This figure is in colour only in the electronic version)

in young children (Mirabell *et al* 2002, Yuh *et al* 2004, St Clair *et al* 2004), and recently Mu *et al* (2005) showed it to be slightly superior to electron therapy.

8.2. Future technology for electron therapy

There are a number of enhancements to electron therapy that should allow it to be used more efficiently and effectively, perhaps offering dose distributions superior to IMXT. Leavitt *et al* (1989b) developed a prototype eMLC for electron arc therapy that improved dose homogeneity in the chest wall through the equivalent of intensity modulation along the arc (Leavitt *et al* 1989a). Subsequently, eMLCs for fixed beams have been investigated by Ma *et al* (2000), Lee *et al* (2000) and Ravindran *et al* (2002). Hogstrom *et al* (2004) proposed a multipurpose, retractable design for the clinic (cf figure 10(a)), which could lead to an accessory-less radiation therapy machine, more efficient delivery of mixed-beam therapy and intensity-modulated electron therapy (IMET). However, eMLC capability from the manufacturer is impeded by its high potential cost and the uncertainty of exactly how to deal with potential patient collision should it be located near the patient surface as are present electron collimating systems. Solutions to the latter might require utilization of helium in the treatment head so as to minimize multiple Coulomb scatter and allow the MLC to be placed further from the patient (Karlsson *et al* 1999).

By also modulating the energy, Ma and colleagues have shown how modulated electron therapy (MET) can be used to treat intact breast (Ma *et al* 2000, 2003) (cf figure 10(b)). Early electron radiation therapy often required adding a small fraction of x-ray beams to spare the skin surface, to improve PTV dose homogeneity and to be able to treat slightly deeper than R_{90} of the maximum electron energy (typically 20 MeV). Mu *et al* (1997) have demonstrated the potential improvement of mixed electron and IMXT beams over IMXT alone. Hence, the utilization of optimized intensity-modulated mixed-beam therapy (IMXT plus MET) remains an important topic worthy of further study.

Another interesting field of research is the use of laser-particle accelerators for electron beams (Chiu *et al* 2004). Its potential impact might be it becoming a more economical accelerator as opposed to offering new clinical techniques. Kainz *et al* (2004) have shown the physical challenges for that technology to evolve further.

Acknowledgments

The authors wish to acknowledge former Chairs of the Department of Radiation Oncology at M D Anderson, the late Gilbert Fletcher and Lester Peters, whose interest in the clinical utilization of electron beams stimulated its development at M D Anderson and throughout the world. Many radiation oncologists at M D Anderson contributed to its development, but none as greatly as the late Norah duV Tapley. Their leadership in developing electron beam therapy for the maximal benefit of the patient and their support for medical physics was essential to the contributions of these authors and their electron beam research colleagues.

References

Abe M and Takahashi M 1981 Intraoperative therapy, the Japanese experience *Int. J. Radiat. Oncol. Biol. Phys.* **7** 863

Able C M, Mills M D, McNeese M D and Hogstrom K R 1991 Evaluation of a total scalp electron irradiation technique *Int. J. Radiat. Oncol. Biol. Phys.* **21** 1063–72

Akazawa C 1989 Treatment of the scalp using photon and electron beams *Med. Dosim.* **14** 129–31

Almond P R 1967 The physical measurements of electron beams from 6 to 18 MeV: absorbed dose and energy calibration *Phys. Med. Biol.* **12** 13–24

Almond P R 1976 Radiation physics of electron beams *Clinical Applications of the Electron Beam* ed N V Tapley (New York: Wiley) pp 7–80

Almond P R 1987 Total skin/electron irradiation technique and dosimetry *Radiation Oncology Physics (Medical Physics Monograph* no 15*)* ed J Kereiakes, H R Elson and C G Born (New York: AIP) pp 296–332

Almond P R, Attix F H, Humphries L J, Kubo H, Nath R, Goetsch S and Rogers D W 1994 The calibration and use of plane-parallel ionization chambers for dosimetry of electron beams: an extension of the 1983 AAPM protocol report of AAPM Radiation Therapy Committee Task Group No. 39 *Med. Phys.* **21** 1251–60

Almond P R, Biggs P J, Coursey B M, Hanson W F, Huq M S, Nath R and Rogers D W O 1999 AAPM's TG-51 protocol for clinical reference dosimetry of high-energy photon and electron beams *Med. Phys.* **26** 1847–70

American Association of Physicists in Medicine (AAPM) 1978 *Practical Aspects of Electron Beam Treatment Planning (Medical Physics Monograph* no 2*)* ed C G Orton and F Bagne (New York: AIP)

American Association of Physicists in Medicine (AAPM) 1983 *Advances in Radiation Therapy Treatment Planning (Medical Physics Monograph* no 9*)* ed A E Wright and A L Boyer (New York: AIP)

American Association of Physicists in Medicine (AAPM) 1987 Total skin electron therapy: technique and dosimetry *AAPM Report* no 23 (New York: AIP)

American Association of Physicists in Medicine Task Group 21, Radiation Therapy Committee (AAPM TG-21) 1983 A protocol for the determination of absorbed dose from high-energy photon and electron beams *Med. Phys.* **10** 741–71

Antolak J A, Bieda M R and Hogstrom K R 2002 Using Monte Carlo methods to commission electron beams: a feasibility study *Med. Phys.* **29** 771–86

Antolak J A, Cundiff J H and Ha C S 1998 Utilization of thermoluminescent dosimetry in total skin electron beam radiotherapy of mycosis fungoides *Int. J. Radiat. Oncol. Biol. Phys.* **40** 101–8

Antolak J A, el-Katib E and Scrimger J W 1993 Verification of a two-dimensional pencil-beam arc electron dose calculation algorithm *Med. Phys.* **20** 1735–42

Antolak J A and Hogstrom K R 1998 Multiple scattering theory for total skin electron beam design *Med. Phys.* **25** 851–9

Archambeau J O, Forrell B, Doria R, Findley D O, Jurisch R and Jackson R 1981 Use of variable thickness bolus to control electron beam penetration in chest wall irradiation *Int. J. Radiat. Oncol. Biol. Phys.* **7** 835–42

Aucouturier J, Huber H and Jaouen J 1970 Systeme de transport du faisceau d'electrons dans le sagittaire *Rev. Tech. Thomson-CSF* **2** 655

Beach J L, Coffey C W and Wade J S 1981 Individualized chest wall compensating bolus for electron irradiation following mastectomy: an ultrasound approach *Int. J. Radiat. Oncol. Biol. Phys.* **7** 1607–11

Beck C 1909 External roentgen treatment of internal structures (eventration treatment) *N. Y. Med. J.* **89** 621–2

Beddar A S and Krishnan S 2005 Intraoperative radiotherapy using a mobile electron LINAC: a retroperitoneal sarcoma case *J. Appl. Clin. Med. Phys.* **6** 95–107

Berger M J and Seltzer S M 1969a Quality of radiation in a water medium irradiated with high-energy electron beams *Abstracts 12th Int. Cong. Radiology (Tokyo)* p 127

Berger M J and Seltzer S M 1969b Calculation of energy and charge deposition and of the electron flux in a water medium bombarded with 20-MeV electrons *Ann. N. Y. Acad. Sci.* **161** 8–23

Bethe H A and Ashkin J 1953 Part II: passage of radiations through matter *Experimental Nuclear Physics* vol 1 ed E Segré (New York: Wiley) pp 166–357
Biggs P J 1984 The effect of beam angulation on central axis per cent depth dose for 4–29 MeV electrons *Phys. Med. Biol.* **29** 1089–96
Biggs P J, Boyer A L and Doppke K P 1979 Electron dosimetry of irregular fields on the Clinac-18 *Int. J. Radiat. Oncol. Biol. Phys.* **5** 433–40
Biggs P J, Epp E R, Ling C C, Novack D H and Michaels H B 1981 Dosimetry, field shaping and other considerations for intra-operative electron therapy *Int. J. Radiat. Oncol. Biol. Phys.* **7** 875–84
Blomquist M, Karlsson M and Karlsson M 1996 Test procedures for verification of an electron pencil beam algorithm implemented for treatment planning *Radiother. Oncol.* **39** 271–86
Boag J W 1950 Ionization measurements at very high intensities *Br. J. Radiol.* **23** 601–11
Boag J W 1966 *Radiation Dosimetry* vol 2 ed F H Attix and W C Roesch (New York: Academic)
Boag J W 1982 The recombination correction for an ionization chamber exposed to pulsed radiation in a 'swept beam' technique *Phys. Med. Biol.* **27** 201–21
Boag J W and Currant J 1980 Current collection and ionic recombination in small cylindrical ionization chambers exposed to pulsed radiation *Br. J. Radiol.* **53** 471–8
Boone M L M, Almond P R and Wright A E 1969 High energy electron dose perturbations in regions of tissue heterogeneity in high energy radiation therapy dosimetry *Ann. N. Y. Acad. Sci.* **161** 214–32
Bova F J 1990 A film phantom for routine film dosimetry in the clinical environment *Med. Dosim.* **15** 83–5
Boyd R A, Hogstrom K R, Antolak J A and Shiu A S 2001a A measured data set for evaluating electron-beam dose algorithms *Med. Phys.* **28** 950–8
Boyd R A, Hogstrom K R and Rosen I I 1998 Effect of using an initial polyenergetic spectrum with the pencil-beam redefinition algorithm for electron-dose calculations in water *Med. Phys.* **25** 2176–85
Boyd R A, Hogstrom K R and Starkschall G 2001b Electron pencil-beam redefinition algorithm dose calculations in the presence of heterogeneities *Med. Phys.* **28** 2096–104
Brahme A 1975 Investigations on the application of a microtron accelerator for radiation therapy *PhD Dissertation* Department of Medical Radiation Physics at Karolinska Institute and Stockholm University
Brahme A 1977 Electron transport phenomena and absorbed dose distributions in therapeutic electron beams *Book of Abstracts XIV: International Congress of Radiology (Rio de Janeiro)* p 198
Brahme A 1981 Electron beam dose planning using Gaussian beams: mathematical background *Acta Radiol. Oncol.* **20** 147–58
Brahme A 1983 Geometric parameters of clinical electron beams *Acta Radiol. Suppl.* **364** 11–9
Brahme A 1985 Current algorithms for computed electron beam dose planning *Radiother. Oncol.* **3** 347–62
Brahme A and Reistad D 1981 *IEEE Trans. Nucl. Sci.* **28** 2
Brahme A and Svensson H 1976 Specification of electron beam quality from the central-axis depth absorbed-dose distribution *Med. Phys.* **3** 95–102
Brown F B *et al* 2002 MCNP version 5 *Trans. Am. Nucl. Soc.* **87** 273
Bruinvis I A D, Van Amstel A, Elevelt A J and Van der Laarse R 1983 Calculation of electron beam dose distributions for arbitrarily shaped fields *Phys. Med. Biol.* **28** 667–83
Cheng A, Harms W B, Gerber R L and Wong J W 1996 Systematic verification of a three-dimensional electron beam dose calculation algorithm *Med. Phys.* **23** 685–93
Chi P M 2004 A three-dimensional pencil-beam redefinition algorithm for electron arc therapy *MS Thesis* University of Texas Health Science Center
Chi P M, Hogstrom K R, Starkschall G, Antolak J A and Boyd R A 2005 Modeling skin collimation using the electron pencil beam redefinition algorithm *Med. Phys.* **32** 3409–18
Chi P M, Hogstrom K R, Starkschall G, Boyd R A, Tucker S L and Antolak J A 2006 Application of the electron pencil beam redefinition algorithm to electron arc therapy *Med. Phys.* **33** at press
Chiu C, Fomytskyi M, Grigsby F, Raischel F, Downer M C and Tajima T 2004 Laser electron accelerators for radiation medicine: a feasibility study *Med. Phys.* **31** 2042–52
Crosby E H, Almond P R and Shalek R J 1966 Energy dependence of lithium fluoride dosemeters at high energies *Phys. Med. Biol.* **11** 131–2
Cygler J E, Daskalov G M, Chan G H and Ding G X 2004 Evaluation of the first commercial Monte Carlo dose calculation engine for electron beam treatment planning *Med. Phys.* **31** 142–53
Desai K R *et al* 1988 Total skin electron irradiation for mycosis fungoides: relationship between acute toxicities and measured dose at different anatomic sites *Int. J. Radiat. Oncol. Biol. Phys.* **15** 641–5
Deutsches Institute für Normung (DIN) 1996 Dosismessverfahren nach der Sondenmethode fur Photonen-und Elektronenstrahlung-Ionisationsimetrie *Deutsche Norm* DIN 6800, Teil 2, Berlin
Dewit L, Van Dam J, Rijinders A, van de Velde G, Ang K K and van der Schueren E 1984 A modified radiotherapy technique in the treatment of medulloblastoma *Int. J. Radiat. Oncol. Biol. Phys.* **10** 231–41

Ding G X and Rogers D W 1996 Mean energy, energy-range relationships and depth-scaling factors for clinical electron beams *Med. Phys.* **23** 361–76

Ding G X, Rogers D W, Cygler J W and Mackie T R 1997 Electron fluence correction factors for conversion of dose in plastic to dose in water *Med. Phys.* **24** 161–76

Ding G X, Rogers D W and Mackie T R 1995 Calculation of stopping-power ratios using realistic clinical electron beams *Med. Phys.* **22** 489–501

du Plessis F C P, Willemse C A, Lötter M G and Goedhals L 1998 The indirect use of CT numbers to establish material properties needed for Monte Carlo calculation of dose distributions in patients *Med. Phys.* **25** 1195–201

Dutreix J and Dutreix A 1969 Film dosimetry of high-energy electrons *Ann. N. Y. Acad. Sci.* **161** 33–43

Duvic M, Apisarnthanarax N, Cohen D S, Smith T L, Ha C S and Kurzrock R 2003 Analysis of long-term outcomes of combined modality therapy for cutaneous T-cell lymphoma *J. Am. Acad. Dermatol.* **49** 35–49

Duvic M, Lemak N A, Redman J R, Eifel P J, Tucker S L, Cabanillas F F and Kurzrock R 1996 Combined modality therapy for cutaneous T-cell lymphoma *J. Am. Acad. Dermatol.* **34** 1022–9

Edelstein G R, Clark T and Holt J G 1973 Dosimetry for total-body electron-beam therapy in the treatment of mycosis fungoides *Radiology* **108** 691–4

Ekstrand K E and Dixon R L 1982 The problem of obliquely incident beams in electron-beam treatment planning *Med. Phys.* **9** 276–8

Eyges L 1948 Multiple scattering with energy loss *Phys. Rev.* **74** 1534–5

Fields R S and Hogstrom K R 1982 A computer model for combining electron and photon beams *Proc. Electron Dosimetry and Arc Therapy Symposium* ed B Paliwal (New York: AIP) pp 161–80

Fields R S and Hogstrom K R 1984 Optimization of electron–photon mixed beam planning. *Proc. 8th Int. Conf. on the Use of Computers in Radiation Therapy* (Silver Spring, MD: IEEE Computer Society Press) pp 248–54

Fippel M, Kawrakow I and Friedrich K 1997 Electron beam dose calculations with the VMC algorithm and the verification data of the NCI working group *Phys. Med. Biol.* **42** 501–20

Fraass B A, Miller R W, Kinsella T J, Sindelar W F, Harringtron F S, Yeakel K, van de Geijn J and Glatstein E 1985 Intraoperative radiation therapy at the National Cancer Institute: technical innovations and dosimetry *Int. J. Radiat. Oncol. Biol. Phys.* **11** 1299–311

Fraass B A, Robertson P L and Glatstein E 1983 Whole-skin electron treatment: patient skin dose distribution *Radiol.* **146** 811–4

Goede M R, Gooden D S, Ellis R G and Brickner T J 1977 A versatile electron collimation system to be used with electron cone supplied with Varian's Clinac *Int. J. Radiat. Oncol. Biol. Phys.* **2** 791–5

Gray L H 1936 Ionization method for the absolute measurement of gamma-ray energy *Proc. R. Soc.* A **156** 578

Green A D 1991 Modeling of dual foil scattering systems for clinical electron beams *MS Thesis* University of Texas Health Science Center

Greene M H, Dalager N A, Lamber S I, Argyropoulos C E and Fraumen J F Jr 1979 Mycosis fungoides: epidemiologic observations *Cancer Treat. Rep.* **63** 597–606

Grusell E, Montelius A, Brahme A, Rikner G and Russell K 1994 A general solution to charged particle beam flattening using an optimized dual-scattering-foil technique, with application to proton therapy beams *Phys. Med. Biol.* **39** 2201–16

Gund K and Paul W 1950 Experiments with a 6-MeV betatron *Nucleonics* **7** 36–45

Harder D 1965 Energiespektren schneller Elekronen in verschiedenen Tiefen *Symp. on High-Energy Electrons* ed A Zuppinger and G Poretti (Berlin: Springer) p 260

Hettinger G and Pettersson C 1965 Determination of Frick *G*-value for 30 MeV electrons with the use of a calorimetric technique *Symp. on High-Energy Electrons (Montreaux, Switzerland)* ed A Zuppinger and G Poretti (Berlin: Springer) pp 57–61

Hogstrom K R 1983a Implementation of CT treatment planning *Advances in Radiation Therapy Treatment Planning* ed A E Wright and A L Boyer (New York: AAPM) pp 268–81

Hogstrom K R 1983b Dosimetry of electron heterogeneities *Advances in Radiation Therapy Treatment Planning (Medical Physics Monograph* no 9*)* ed A Wright and A Boyer (New York: AIP) pp 223–43

Hogstrom K R 1991 Treatment planning in electron-beam therapy *Frontiers in Radiation Therapy Oncology: The Role of High Energy Electrons in the Treatment of Cancer* ed J M Vaeth and J L Meyer (Farmington, CT: Karger) pp 30–52

Hogstrom K R 2004 Electron beam therapy: dosimetry, planning, and techniques *Principles and Practice of Radiation Oncology* ed C Perez *et al* (Baltimore, MD: Lippincott, Williams & Wilkins) pp 252–82

Hogstrom K R and Almond K R 1982 The effect of electron multiple scattering on dose measured in non-water phantoms *Med. Phys.* **9** 607

Hogstrom K R, Antolak J A, Kudchadker R J, Ma C M and Leavitt D D 2003 Modulated electron therapy *Intensity Modulated Radiation Therapy, The State of the Art: Proc. 2003 AAPM Summer School* ed J Palta and R Mackie (Madison, WI: Medical Physics Publishing) pp 749–86

Hogstrom K R, Boyd R A, Antolak J A, Svatos M M, Faddegon B A and Rosenman J G 2004 Dosimetry of a prototype retractable eMLC for fixed-beam electron therapy *Med. Phys.* **31** 443–60

Hogstrom K R, Boyer A L, Shiu A S, Ochran T G, Kirsner S M, Krispel F and Rich T 1990 Design of metallic electron beam cones for an intraoperative therapy linear accelerator *Int. J. Radiat. Oncol. Biol. Phys.* **18** 1223–32

Hogstrom K R, Ewton J R, Cundiff J H, Ames J C and McNeese M D 1984a Beam delivery system and dosimetry for total skin electron therapy at MDAH *Med. Phys.* **11** 389

Hogstrom K R and Fields R S 1983 Use of CT in electron beam treatment planning: current and future development *Computed Tomography in Radiation Therapy* ed C C Ling (New York: Raven) pp 241–52

Hogstrom K R, Kurup R G, Shiu A S and Starkschall G 1989 A two-dimensional pencil-beam algorithm for calculation of arc electron dose distributions *Phys. Med. Biol.* **34** 315–41

Hogstrom K R and Leavitt D 1987 Dosimetry of electron arc therapy *Radiation Oncology Physics 1986: Proc. 1986 Summer School of the AAPM* ed H Elson and C Born (New York: AIP) pp 265–95

Hogstrom K R, Meyer J A and Melson R 1985 Variable electron collimator for the Mevatron 77 design and dosimetry *Proc. Conf. of 1985 Mevatron Users (Hilton Head, SC)* pp 251–76

Hogstrom K R, Mills M D and Almond P R 1981 Electron beam dose calculations *Phys. Med. Biol.* **26** 445–59

Hogstrom K R, Mills M D, Meyer J A, Palta J R, Mellenberg D E, Meoz R T and Fields R S 1984b Dosimetric evaluation of a pencil-beam algorithm for electrons employing a two-dimensional heterogeneity correction *Int. J. Radiat. Oncol. Biol. Phys.* **10** 561–9

Hogstrom K R and Steadham R S 1996 Electron beam dose computation *Teletherapy: Present and Future. 1996 Proc. Summer School of the AAPM* ed J Palta and T R Mackie (Madison, WI: Advanced Medical Publishing) pp 137–74

Hogstrom K R, Steadham R E, Wong P F and Shiu A S 2000 Monitor unit calculations for electron beams *Monitor Unit Calculations for External Photon and Electron Beams* ed J P Gibbons (Middleton, WI: Advanced Medical Publishing) pp 113–25

Holt J G, Buffa A, Perry D J, McDonald J C and Chang I 1979 Absorbed dose measurements using parallel plate polystyrene ionization chambers in polystyrene phantoms *Int. J. Radiol. Oncol. Biol.* **5** 2031–44

Holt J F and Perry D J 1982 Some physical consideration in whole skin electron beam therapy *Med. Phys.* **9** 769–76

Hoppe R T 2003 Mycosis fungoides radiation therapy *Dermatol. Ther.* **16** 347–54

Huizenga H and Storchi P R M 1987 The in-air scattering of clinical electron beams as produced by accelerators with scanning beams and diaphragm collimators *Phys. Med. Biol.* **32** 1011–29

Huizenga H and Storchi P R M 1989 Numerical calculation of energy deposition by broad high-energy electron beams *Phys. Med. Biol.* **34** 1371–96

Institution of Physics and Engineering in Medicine and Biology (IPEMB) 1996 The IPEMB code of practice for electron dosimetry for radiotherapy beams of initial energy from 2 to 5 MeV based on an air-kerma calibration *Phys. Med. Biol.* **41** 2557

International Atomic Energy Agency (IAEA) 1968 *Directory of High Energy Radiotherapy Center* ed P Pfalzner (Vienna: International Atomic Energy Agency)

International Atomic Energy Agency (IAEA) 1987 Absorbed dose determination in photon and electron beams: an international code of practice *Technical Report Series* no 277 (Vienna: International Atomic Energy Agency)

International Atomic Energy Agency (IAEA) 1997 The use of plane parallel ionization chambers in high energy electron and photon beams: an international code of practice for dosimetry *Technical Report Series* no 381 (Vienna: International Atomic Energy Agency)

International Commission on Radiation Units and Measurements (ICRU) 1972 Radiation Dosimetry: Electrons with Initial Energies Between 1 and 50 MeV *ICRU Report* 21 (Bethesda, MD: International Commission on Radiation Units and Measurements)

International Commission on Radiation Units and Measurements (ICRU) 1984 Radiation Dosimetry: Electron Beams with Energies Between 1 and 50 MeV *ICRU Report* 35 (Bethesda, MD: International Commission on Radiation Units and Measurements)

Janssen J J, Riedeman D E J, Morawska-Kaczynska M, Storchi P R M and Huizenga H 1994 Numerical calculation of energy deposition by high-energy electron beams: III. Three-dimensional heterogeneous media *Phys. Med. Biol.* **39** 1351–66

Jeraj R, Keall P J and Ostwald P M 1999 Comparisons between MCNP, EGS4 and experiment for clinical electron beams *Phys. Med. Biol.* **44** 705–17

Jette D 1995 Electron beam dose calculations *Radiation Therapy Physics* ed A R Smith (Berlin: Springer) pp 95–121

Jette D and Walker S 1992 Electron dose calculation using multiple-scattering theory: evaluation of a new model for inhomogeneities *Med. Phys.* **19** 1241–54

Jones D 1991 Apparatus, technique and dosimetry of intraoperative electron beam therapy *The Role of High Energy Electrons in the Treatment of Cancer: 25th Annual San Francisco Cancer Symposium (February 1990) (Frontiers of Radiation Therapy and Oncology* vol 25*)* ed J L Meyer and J M Vaeth (Basle: Karger) pp 233–45

Kainz K K, Antolak J A, Almond P R, Bloch C D and Hogstrom K R 2005 Dual scattering foil design for poly-energetic electron beams *Phys. Med. Biol.* **50** 755–67

Kainz K K, Hogstrom K R, Antolak J A, Almond P R, Bloch C D, Chiu C, Fomytskyi M, Raischel F, Downer M and Tajima T 2004 Dose properties of a laser accelerated electron beam and prospects for clinical application *Med. Phys.* **31** 2053–67

Kapur A, Ma C M, Mok E C, Findley D O and Boyer A L 1998 Monte Carlo calculations of electron beam output factors for a medical linear accelerator *Phys. Med. Biol.* **43** 3479–94

Karlsson M G, Karlsson M and Ma C M 1999 Treatment head design for multileaf collimated high-energy electrons *Med. Phys.* **26** 2161–7

Karzmark C J, Loevinger R, Steele R E and Weissbluth M 1960 A technique for large-field superficial electron therapy *Radiology* **74** 633–44

Karzmark C J and Morton R J 1989 *Primer on Theory and Operation of Linear Accelerators in Radiation Therapy* 2nd edn (Madison, WI: Medical Physics Publishing)

Karzmark C J, White J and Fowler J T 1964 Lithium fluoride thermoluminescent dosimetry *Phys. Med. Biol.* **9** 3273–88

Kawachi K 1975 Calculation of electron dose distribution for radiotherapy treatment planning *Phys. Med. Biol.* **20** 571–7

Kawrakow I, Fippel M and Friedrich K 1996 3D electron dose calculation using a voxel based Monte Carlo algorithm (VMC) *Med. Phys.* **23** 445–57

Keall P J and Hoban P W 1996 Super-Monte Carlo: a 3D electron beam dose calculation algorithm *Med. Phys.* **23** 2023–34

Khan F 2003 *The Physics of Radiation Therapy* 3rd edn (Philadelphia, PA: Lippincott, Williams & Wilkins)

Khan F M, Doppke K P, Hogstrom K R, Kutcher G J, Nath R, Prasad S C, Purdy J A, Rozenfeld M and Werner B L 1991 Clinical electron-beam dosimetry: report of AAPM Radiation Therapy Committee Task Group No. 25 *Med. Phys.* **18** 73–109

Khan F M, Fullerton G D, Lee J M, Moore V C and Levitt S H 1977 Physical aspects of electron-beam arc therapy *Radiology* **124** 497–500

Khan F M, Higgins P D, Gerbi B J, Deibel F C, Sethi A and Mihailidis D N 1998 Calculation of depth dose and dose per monitor unit for irregularly shaped electron fields *Phys. Med. Biol.* **43** 2741–54

Khan F M, Sewchand W and Levitt S H 1978 Effect of air space on depth dose in electron beam therapy *Radiology* **126** 249–51

Klein E E, Low D A and Purdy J A 1995 Changes in electron beam dosimetry with a new scattering foil-applicator system on a CL2100C *Int. J. Radiat. Oncol. Biol. Phys.* **32** 483–90

Klevenhagen S C 1978 Behavior of p–n junction silicon detectors in a temperature-compensated direct-current circuit *Med. Phys.* **5** 52–65

Klevenhagen S C 1985 Physics of electron beam therapy *Medical Physics Handbook* vol 13 (Boston, MA: Hilger)

Klevenhagen S C 1993 *Physics and Dosimetry of Therapy Electron Beams* (Madison, WI: Medical Physics Publishing)

Klevenhagen S C, Lambert G D and Arbabi A 1982 Backscattering in electron beam therapy for energies between 3 and 35 MeV *Phys. Med. Biol.* **27** 363–73

Korevaar E W, Dabrowski R, Janssen J J, Storchi P R M and Huizenga H 1996 Phase space evolution distribution functions for high electron beams *Phys. Med. Biol.* **41** 2079–90

Kozlov A P and Shishov V A 1976 Forming of electron beams from a betatron by foil scatterers *Acta Radiol. Ther. Phys. Biol.* **15** 493–512

Kudchadker R J, Antolak J A, Morrison W H, Wong P F and Hogstrom K R 2003 Utilization of custom electron bolus in head and neck radiotherapy *J. Appl. Clin. Med. Phys.* **4** 321–33

Kudchadker R J, Hogstrom K R, Garden A S, McNeese M D and Boyd R A 2002 Electron conformal radiotherapy using bolus and intensity modulation *Int. J. Radiat. Oncol. Biol. Phys.* **53** 1023–37

Kurup R G, Hogstrom K R, Otte V A, Moyers M F, Tung S and Shiu A S 1992 Dosimetric evaluation of a two-dimensional, arc electron, pencil-beam algorithm in water and PMMA *Phys. Med. Biol.* **37** 127–44

Lam K S, Lam W C, O'Neill M J, Lee D J and Zeinreich E 1987 Electron arc therapy: beam data requirements and treatment planning *Clin. Radiol.* **38** 379–83

Lambert G D and Klevenhagen S C 1982 Penetration of backscattered electrons in polystyrene for energies between 1 and 25 MeV *Phys. Med. Biol.* **27** 721–5

Laughlin J S 1965 Calorimetric determination of absorbed dose with electrons *Symp. on High-Energy Electrons (Montreaux, Switzerland)* ed A Zuppinger and G Poretti (Berlin: Springer) pp 65–71

Laughlin J S, Ovadia J, Beattie J W, Henderson W J, Harvey R A and Haas L L 1953 Some physical aspects of electron beam therapy *Radiology* **60** 165–85

Lax I, Brahme A and Andreo P 1983 Electron dose planning using Gaussian beams. Improved dose profiles *Acta Radiol. Suppl.* **364** 49–59

Leavitt D D, Earley L and Stewart J R 1990a Design and production of customized field shaping devices for electron arc therapy *Med. Dosim.* **15** 25–31

Leavitt D D, Peacock L M, Gibbs F A Jr and Stewart J R 1985 Electron arc therapy: physical measurement and treatment planning techniques *Int. J. Radiat. Oncol. Biol. Phys.* **11** 987–99

Leavitt D D, Stewart J R and Earley L 1990b Improved dose homogeneity in electron arc therapy achieved by a multiple energy technique *Int. J. Radiat. Oncol. Biol. Phys.* **19** 159–65

Leavitt D D, Stewart J R, Moeller J H and Earley L 1989a Optimization of electron arc therapy doses by multi-vane collimator control *Int. J. Radiat. Oncol. Biol. Phys.* **16** 489–96

Leavitt D D, Stewart J R, Moeller J H, Lee W L and Takach G A Jr 1989b Electron arc therapy: design, implementation and evaluation of a dynamic multi-vane collimator system *Int. J. Radiat. Oncol. Biol. Phys.* **17** 1089–94

Lee C T, Bilton S D, Famiglietti R M, Riley B A, Mahajan A, Chang E L, Maor M H, Woo S Y, Cox J D and Smith A R 2005 Treatment planning with protons for pediatric retinoblastoma, medulloblastoma, and pelvic sarcoma: how do protons compare with other conformal techniques? *Int. J. Radiat. Oncol. Biol. Phys.* **63** 362–72

Lee M C, Jiang S B and Ma C M 2000 Monte Carlo and experimental investigations of multileaf collimated electron beams for modulated electron radiation therapy *Med. Phys.* **27** 2708–18

Lee N, Puri D R, Blanco A L and Chao K S 2005 Intensity-modulated radiation therapy in head and neck cancers: an update *Head Neck* at press

Lillicrap S C, Wilson P and Boag J 1975 Dose distributions in high energy electron beams: production of broad beam distributions from narrow beam data *Phys. Med. Biol.* **20** 30–8

Ling C C, Rogers C C and Morton R J (ed) 1983 *Computed Tomography in Radiation Therapy* (New York: Raven)

Locke J, Low D A, Grigirett T and Chao K S C 2002 Potential of tomotherapy for total scalp treatment *Int. J. Radiat. Oncol. Biol. Phys.* **52** 553–9

Loevinger E, Karzmark C J and Weissbluth M 1961 Radiation therapy with high-energy electrons *Radiology* **77** 906

Low D A, Starkschall G, Bujnowski S W, Wang L L and Hogstrom K R 1992 Electron bolus design for radiotherapy treatment planning: bolus design algorithms *Med. Phys.* **19** 115–24

Low D A, Starkschall G, Sherman N E, Bujnowski S W, Ewton J R and Hogstrom K R 1995 Computer-aided design and fabrication of an electron bolus for treatment of the paraspinal muscles *Int. J. Radiat. Oncol. Biol. Phys.* **33** 1127–38

Ma C M, Ding M, Li J S, Lee M C, Pawlicki T and Deng J 2003 A comparative dosimetric study on tangential photon beams, intensity-modulated radiation therapy (IMRT) and modulated electron radiotherapy (MERT) for breast cancer treatment *Phys. Med. Biol.* **48** 909–24

Ma C M, Li J S, Pawlicki T, Jiang S B, Deng J, Lee M C, Koumrian T, Luxton M and Brian S 2002 A Monte Carlo dose calculation tool for radiotherapy treatment and planning *Phys. Med. Biol.* **47** 1671–89

Ma C M, Mok E, Kapur A, Pawlicki T, Findley D, Brain S, Forster K and Boyer A L 1999 Clinical implementation of a Monte Carlo treatment planning system *Med. Phys.* **26** 2133–43

Ma C M, Pawlicki T, Lee M C, Jiang S B, Li J S, Deng J, Yi B, Mok E and Boyer A L 2000 Energy- and intensity-modulated electron beams for radiotherapy *Phys. Med. Biol.* **45** 2293–311

Mackie T R and Battista J J 1984 A macroscopic Monte Carlo method for electron beam dose calculations: a proposal *Proc. 8th Conf. on Use of Computers in Radiation Therapy* (Toronto: IEEE) pp 123–7

Mandour M A, Nüsslin F and Harder D 1983 Characteristic functions of point monodirectional electron beams *Acta Radiol. Suppl.* **364** 43–8

Maor M H, Fields R S, Hogstrom K R and van Eys J 1985 Improving the therapeutic ratio of craniospinal irradiation in medulloblastoma *Int. J. Radiat. Oncol. Biol. Phys.* **11** 687–97

Markus B 1978 A review of 25 years' clinical application of fast electrons in radiotherapy *Strahlentherapie* **154** 221–4

Marre D, Ferreira I H, Bridier A, Bjoreland A, Svensson H and Dutreix A 2000 Energy correction factors of LiF powder TLDs irradiated in high-energy electron beams and applied to mailed dosimetry for quality assurance networks *Phys. Med. Biol.* **45** 3657–74

Marre D and Marinello G 2004 Comparison of p-type commercial electron diodes for *in vivo* dosimetry *Med. Phys.* **31** 50–6

Mattsson L O, Johansson K A and Svensson H 1981 Calibration and use of plane-parallel ionization chambers for the determination of absorbed dose in electron beams *Acta Radiol. Oncol.* **20** 385–99

McCullough E C and Anderson J A 1982 The dosimetric properties of an applicator system for intraoperative electron-beam therapy utilizing a Clinac-18 accelerator *Med. Phys.* **9** 261–8

McNeely L K, Jacobson G M, Leavitt D D and Stewart J R 1988 Electron arc therapy: chest wall irradiation of breast cancer patients *Int. J. Radiat. Oncol. Biol. Phys.* **14** 1287–94

McNutt T R and Tomé W A 2002 A method of scaling the 3D electron pencil-beam dose calculation to obtain accurate monitor units for irregularly-shaped electron beams *Med. Dosim.* **27** 209–13

McShan D L, Fraass B A and Ten Haken R K 1994 Dosimetric verification of a 3D electron pencil beam dose calculation algorithm *Med. Phys.* **21** 13–23

Meurk M L, Goer D A, Spalek G and Cook T 1997 The Mobetron: a new concept for IORT *Intraoperative Radiation Therapy in the Treatment of Cancer: 6th Int. IORT Symposium and 31st San Francisco Cancer Symposium (September 1996) (Frontiers of Radiation Therapy and Oncology* vol 31*)* ed J L Meyer and W Hinkelbein (Basle: Karger) pp 65–70

Meyer J L and Hinkelbein W 1997 *Intraoperative Radiation Therapy in the Treatment of Cancer: 6th Int. IORT Symposium and 31st San Francisco Cancer Symposium (September 1996) (Frontiers of Radiation Therapy and Oncology* vol 31*)* (Basle: Karger)

Meyer J A, Palta J R and Hogstrom K R 1984 Demonstration of relatively new electron dosimetry measurement techniques on the Mevatron 80 *Med. Phys.* **11** 670–7

Meyer J L and Vaeth J M (ed) 1991 *The Role of High Energy Electrons in the Treatment of Cancer: 25th Annual San Francisco Cancer Symposium (February 1990) (Frontiers of Radiation Therapy and Oncology* vol 25*)* (Basle: Karger)

Milan J and Bentley R E 1974 The storage and manipulation of radiation dose data in a small digital computer *Br. J. Radiol.* **47** 115–21

Mills M D, Almond P R, Boyer A L, Ochran T G, Madigan W, Rich T A and Dally E B 1990 Shielding considerations for an operating room based intraoperative electron radiotherapy unit *Int. J. Radiat. Oncol. Biol. Phys.* **18** 1215–21

Mills M D, Fajardo L C, Wilson D L, Daves J L and Spanos W J 2001 Commissioning of a mobile electron accelerator for intraoperative radiotherapy *J. Appl. Clin. Med. Phys.* **2** 121–30

Mills M D, Hogstrom K R and Almond P R 1982 Prediction of electron beam output factors *Med. Phys.* **9** 60–8

Mirabell R, Lomax A, Cella L and Schneider U 2002 Potential reduction of the incidence of radiation-induced second cancers by using proton beams in the treatment of pediatric tumors *Int. J. Radiat. Oncol. Biol. Phys.* **54** 824–9

Mohan R, Bading J, Caley R J, Reid A, Ding J and Laughlin J S 1981 Computerized electron beam dosimetry *Proc. Symp. on Electron Beam Therapy* ed F C H Chu and J S Laughlin (New York: Memorial Sloan-Kettering Cancer Center) pp 75–81

Morris W T and Owen B 1975 An ionization chamber for therapy level dosimetry of electron beams *Phys. Med. Biol.* **20** 718–27

Morrison W H, Wong P F, Starkschall G, Garden A S, Childress C, Hogstrom K R and Peters L J 1995 Water bolus for electron irradiation of the ear canal *Int. J. Radiat. Oncol. Biol. Phys.* **33** 479–83

Mu X, Bjork-Eriksson T, Nill S, Oelfke U, Johansson K A, Gagliardi G, Johansson L, Karlsson M and Zackrisson D B 2005 Does electron and proton therapy reduce the risk of radiation induced cancer after spinal irradiation for childhood medulloblastoma? A comparative treatment planning study *Acta Oncol.* **44** 554–62

Mu X, Olofsson L, Karlsson M, Sjögren R and Zazkrisson B 2004 Can photon IMRT be improved by combination with mixed electron and photon techniques *Acta Oncol.* **43** 727–35

Muller-Runkel R and Cho S H 1997 Evaluation of a commercial three-dimensional electron pencil beam algorithm *Med. Phys.* **24** 91–101

Nederlandse Commissie voor Stralingdosimetrie (NCS) 1990 Code of practice for the dosimetry of high-energy electron beams *Report* NCS-5 (Amsterdam: NCS)

Nelson W R, Hirayama H and Rogers D W O 1985 The EGS4 code system *Stanford Linear Accelerator Center Report* (Stanford: SLAC) p 265

Neuenschwander H and Born E J 1992 A macro Monte Carlo method for electron beam dose calculations *Phys. Med. Biol.* **37** 107–25

Neuenschwander H, Mackie T R and Reckwerdt P J 1995 MMC—a high performance Monte Carlo code for electron beam treatment planning *Phys. Med. Biol.* **40** 543–74

Nordic Association of Clinical Physics (NACP) 1980 Procedures in external radiation therapy dosimetry with electron and photon beams with maximum energies between 1 and 50 MeV *Acta Radiol. Oncol.* **19** 55

Nordic Association of Clinical Physics (NACP) 1983 Electron beams with mean energies at the phantom surface below 15 MeV *Acta Radiol. Oncol.* **20** 403

Nüsslin F 1979 Computerized treatment planning in therapy with fast electrons: a review of procedures for calculation of dose distribution *Medicamundi* **24** 112–8

Nyerick C E, Ochran T G, Boyer A L and Hogstrom K R 1991 Dosimetry characteristics of metallic cones for intraoperative radiotherapy *Int. J. Radiat. Oncol. Biol. Phys.* **21** 501–10

Olivares-Pla M, Podgorsak E B and Pla C 1997 Electron arc dose distributions as a function of beam energy *Med. Phys.* **24** 127–32

Orton N, Jaradat H, Welsh J and Tomé W 2005 Total scalp irradiation using helical tomotherapy *Med. Dosim.* **30** 162–8
Page V, Gardner A and Karzmark C J 1970 Patient dosimetry in the electron treatment of large superficial lesions *Radiology* **94** 635–41
Palos B and Fessenden P 1982 TL dosimetry for treatment of mycosis fungoides with 4 MeV electrons *Med. Phys.* **9** 618
Palta J R, Biggs P J, Hazle J D, Huq M S, Dahl R A, Ochran T G, Soen J, Dobelbower R R Jr and McCullough E C 1995 Intraoperative electron beam radiation therapy: technique, dosimetry, and dose specification: report of Task Force 48 of the Radiation Therapy Committee, American Association of Physicists in Medicine *Int. J. Radiat. Oncol. Biol. Phys.* **33** 725–46
Peacock L M, Leavitt D D, Gibbs F A Jr and Stewart J R 1984 Electron arc therapy: clinical experience with chest wall irradiation *Int. J. Radiat. Oncol. Biol. Phys.* **10** 2149–53
Peñagarícano J, Papanikolaou N, Yan Y, Youssef E and Ratanatharathorn V 2005 Feasibility of cranio-spinal axis radiation with the Hi-Art tomotherapy system *Radiother. Oncol.* **76** 72–8
Perkins G H, McNeese M D, Antolak J A, Buchholz T A, Strom E A and Hogstrom K R 2001 A custom three-dimensional electron bolus technique for optimization of postmastectomy irradiation *Int. J. Radiat. Oncol. Biol. Phys.* **51** 1142–51
Perry D J and Holt J G 1980 A model of calculating the effects of small inhomogeneities on electron beam dose distributions *Med. Phys.* **7** 207–15
Pinkerton A 1969 Comparison of calorimetric and other methods for the determination of absorbed dose *Ann. N. Y. Acad. Sci.* **161** 63–76
Pinkerton A, Laughlin J S and Holt J G 1966 Energy dependence of lithium fluoride dosimetrics and high electron energy *Phys. Med. Biol.* **11** 129–30
Pla M, Podgorsak E B and Pla C 1989 Electron dose rate and photon contamination in electron arc therapy *Med. Phys.* **16** 692–7
Pla M, Podgorsak E B, Pla C, Freeman C R, Souhami L and Guerra J 1991 Physical aspects of the angle-beta concept in electron arc therapy *Int. J. Radiat. Oncol. Biol. Phys.* **20** 1331–9
Popple R, Weinberg R, Antolak J, Brezovich I, Duan J and Pareek P 2005 Evaluation of a commercial macro Monte Carlo electron dose calculation algorithm *Med. Phys.* **32** 2016 (abstract)
Rashid H, Islam M K, Gaballa H, Rosenow U F and Ting J Y 1990 Small-field electron dosimetry for the Philips SL25 linear accelerator *Med. Phys.* **17** 710–14
Ravindran B P, Singh I R R, Brindha S and Sathyan S 2002 Manual multi-leaf collimator for electron beam shaping—a feasibility study *Phys. Med. Biol.* **47** 4389–96
Rich T A 1986 Intraoperative radiotherapy *Radiother. Oncol.* **6** 207–21
Rich T A and Dally E 1985 The Siemens Mevatron ME: an electron beam accelerator dedicated to intraoperative radiation therapy at M D Anderson hospital *Proc. 1985 MEVATRON Users Conference (Hilton Head Island, SC)* pp 8103–15
Rikner G 1983 Silicon diodes as detectors in relative dosimetry of photon, electron and proton radiation fields *PhD Thesis* Uppsala University
Rikner G 1985 Characteristics of a p-Si detector in high energy electron fields *Acta Radiol. Oncol.* **24** 71–4
Roback D M, Khan F M, Gibbons J P and Sethi A 1995 Effective SSD for electron beams as a function of energy and beam collimation *Med. Phys.* **22** 2093–5
Rogers D W, Faddegon B A, Ding G X, Ma C M, We J and Mackie T R 1995 BEAM: a Monte Carlo code to simulate radiotherapy treatment units *Med. Phys.* **22** 503–24
Ruegsegger D R, Lerude S D and Lyle D 1979 Electron-beam arc therapy using a high energy betatron *Radiology* **133** 483–9
Samuelsson A, Hyödynmaa S and Johansson K-A 1998 Dose accuracy check of the 3D electron beam algorithm in a treatment planning system *Phys. Med. Biol.* **43** 1529–44
Schneider W, Bortfield T and Schlegel W 2000 Correlation between CT numbers and tissue parameters needed for Monte Carlo simulations of clinical dose distributions *Phys. Med. Biol.* **45** 459–78
Schröder-Babo P 1983 Determination of the virtual electron source of a betatron *Acta Radiol. Suppl.* **364** 7–10
Shalek R J and Smith C E 1969 Chemical dosimetry for the measurement of high energy photons and electrons *Ann. N. Y. Acad. Sci.* **161** 44–62
Shiu A S and Hogstrom K R 1991 Pencil-beam redefinition algorithm for electron dose distributions *Med. Phys.* **18** 7–18
Shiu A S, Otte V A and Hogstrom K R 1989 Measurement of dose distributions using film in therapeutic electron beams *Med. Phys.* **16** 911–5
Shiu A S, Tung S S, Gastorf R J, Hogstrom K R, Morrison W H and Peters L J 1996 Dosimetric evaluation of lead and tungsten eye shields in electron beam treatment *Int. J. Radiat. Oncol. Biol. Phys.* **35** 599–604

Shiu A S, Tung S S, Hogstrom K R, Wong J W, Gerber R L, Harms W B, Purdy J A, Haken R K T, McShan D L and Fraass B A 1992 Verification data for electron beam dose algorithms *Med. Phys.* **19** 623–36

Shiu A S, Tung S S, Nyerick C E, Ochran T G, Otte V A, Boyer A L and Hogstrom K R 1994 Comprehensive analysis of electron beam central axis dose for a radiotherapy linear accelerator *Med. Phys.* **21** 559–66

Siegbahn E A, Nilsson B, Fernandez-Varea J M and Andreo P 2003 Calculations of electron fluence correction factors using the Monte Carlo code PENELOPE *Phys. Med. Biol.* **48** 1263–75

Sociedad Española de Fisica Medica (SEFM) 1984 Procedimientos Recomendados para la Dosimetria de Fotones y Electrones de Energias Comprendidas entre 1 MeV y 50 MeV en Radiotherapia de Haces Externos *SEFM Publ.* no 1 (Madrid: Comite de Dosimetria en Radioterapia)

Sociedad Española de Fisica Medica (SEFM) 1987 Suplemento al Documento 84-1: Procedimientos recomendados para la dosimetria de fotones y electrones de energies comprendidas entre 1 MeV y 50 MeV en radioterapia de haces externos *Report* SEFM 87-1 (Madrid: SEFM)

Starkschall G, Henkelmann G C and Ang K K 1990 An interactive system for point dose optimization *Int. J. Radiat. Oncol. Biol. Phys.* **18** 957–64

Starkschall G, Shiu A S, Bujnowski S W, Wang L L, Low D A and Hogstrom K R 1991 Effect of dimensionality of heterogeneity correction on the implementation of a three-dimensional electron pencil-beam algorithm *Phys. Med. Biol.* **36** 201–27

St Clair W H, Adams J A, Bues M, Fullerton B C, La Shell S, Kooy H M, Loeffler J S and Tarbell N J 2004 Advantage of protons compared to conventional x-ray or IMRT in the treatment of a pediatric patient with medulloblastoma *Int. J. Radiat. Oncol. Biol. Phys.* **58** 727–34

Steben J D, Ayyangar K and Suntharalingam N 1979 Betatron electron beam characterization for dosimetry calculations *Phys. Med. Biol.* **24** 299–309

Stewart J R, Leavitt D D and Prows J 1991 Electron arc therapy of the chest wall for breast cancer: rationale, dosimetry, and clinical aspects *Front. Radiat. Ther. Oncol.* **25** 134–50

Suntharalingam N and Cameron J R 1969 Thermoluminescent response of lithium fluoride to high-energy electrons *Ann. N. Y. Acad. Sci.* **161** 77–85

Svensson H and Petersson S 1967 Absorbed dose calibration of thimble chambers with high energy electrons at different phantom depths *Ark. Fys.* **34** 377

Tailor R C, Aguirre J F and Hansen W F 1999 RPC experience with TLD output and energy monitoring of radiation therapy beams *Med. Phys.* **26** 1164

Tapley N D 1976 *Clinical Applications of the Electron Beam* (New York: Wiley)

Ten Haken R K, Fraass B A and Jost R J 1987 Practical methods of electron-dose measurement compared to use of the NACP design chamber in water *Med. Phys.* **14** 1060–8

Thwaites D I, DuSautoy A R, Jordan T, McEwen M R, Nisbet A, Nahum A E and Pitchford W G 2003 The IPEM code of practice for electron dosimetry for radiotherapy beams of initial energy from 4 to 25 MeV based on an absorbed dose to water calibration *Phys. Med. Biol.* **48** 2929–70

Trump J G 1964 Radiation for therapy: in retrospect and prospect *Am. J. Roentgenol. Radium Ther. Nucl. Med.* **91** 22–30

Trump J G, Wright K A, Evans W W, Anson J H, Hare H F, Fromer J L, Jacque F and Horned K W 1953 High energy electrons for the treatment of extensive superficial malignant lesions *Am. J. Radiol.* **69** 623–9

Tung S S, Shiu A S, Starkschall G, Morrison W H and Hogstrom K R 1993 Dosimetric evaluation of total scalp irradiation using a lateral electron–photon technique *Int. J. Radiat. Oncol. Biol. Phys.* **27**

van Battum L J, van der Zee W and Huizenga H 2003 Scattered radiation from applicators in clinical electron beams *Phys. Med. Biol.* **48** 2493–507

van de Geijn J, Chin B, Pochobradsky J and Miller R W 1987 A new model for computerized clinical electron beam dosimetry *Med. Phys.* **14** 577–84

van der Zee W, Hogenbirk A and van der Marck S C 2005 ORANGE: a Monte Carlo dose engine for radiotherapy *Phys. Med. Biol.* **50** 625–41

Verhaegan F, Buffa F M and Deehan C 2001a Quantifying effects of lead shielding in electron beams: a Monte Carlo study *Phys. Med. Biol.* **46** 757–69

Verhaegan F, Mubata C, Pettingell J, Bidmead A M, Rosenburg I, Mockridge D and Nahum A E 2001b Monte Carlo calculation of output factors for circular, rectangular, and square fields of electron accelerators (6–20 MeV) *Med. Phys.* **28** 938–49

Weaver R D, Gerbi B J and Dusenberry K E 1995 Evaluation of dose variation during total skin electron irradiation using thermoluminescent dosimeters *Int. J. Radiat. Oncol. Biol. Phys.* **33** 475–8

Weinhous M S and Meli J A 1984 Determining the correction function for recombination losses in an ionization chamber *Med. Phys.* **11** 846–55

Werner B L, Khan F M and Deibel F C 1982 A model for calculating electron beam scattering in treatment planning *Med. Phys.* **9** 180–7

Wooden K K, Hogstrom K R, Blum P, Gastorf R J and Cox J D 1996 Whole-limb irradiation of the lower calf using a six-field electron technique *Med. Dosim.* **21** 211–8

Ye S J, Pareek P N, Spencer S, Duan J and Brezovich I A 2005 Monte Carlo techniques for scattering foil design and dosimetry in total skin electron irradiations *Med. Phys.* **32** 1460–8

Ysebaert L, Truc G, Dalac S, Lambert D, Petrella T, Barillot I, Naudy S, Horiot J and Maingon P 2004 Ultimate results of radiation therapy for T1–T2 mycosis fungoides (including reirradiation) *Int. J. Radiat. Oncol. Biol. Phys.* **58** 1128–34

Yuh G E, Loredo L N, Yonemoto L T, Bush D A, Shahnazi K, Preston W, Slater J M and Slater J D 2004 Reducing toxicity from craniospinal irradiation: using proton beams to treat medulloblastoma in young children *Cancer J.* **10** 386–90

Zackrisson B and Karlsson M 1996 Matching of electron beams for conformal therapy of target volumes at moderate depths *Radiother. Oncol.* **39** 261–70

Zhang G G, Rogers D W O, Cygler J E and Mackie T R 1999 Monte Carlo investigation of electron beam output factors versus size of square cutout *Med. Phys.* **26** 743–50

Biography

Kenneth R Hogstrom, PhD, DABR, received his BS and MS in physics from the University of Houston and his PhD in physics (nuclear) from Rice University. From 1976 to 1979, Dr Hogstrom was a Research Scientist at the University of New Mexico, working on the pion therapy project in Los Alamos. From 1979 to 1985, he was a faculty member in the Department of Physics at The University of Texas M D Anderson Cancer Center in Houston, working under Dr Peter Almond. This resulted in his interest and early contributions to electron beam physics and dosimetry. From 1985 to 2001, Dr Hogstrom served as Chair of the Department of Radiation Physics at the M D Anderson Cancer Center, and in 2004 he retired as Professor Emeritus. Dr Hogstrom served as Director of Medical Physics Programs at The University of Texas Graduate School of Biomedical Sciences at Houston for 20 years. Dr Hogstrom is a Fellow of the AAPM and ACMP and served as AAPM President in 2000. He received the AAPM Coolidge Award in 2003 and the ACMP Marvin M D Williams Award in 2004. Currently, he is Professor and Director of the Medical Physics and Health Physics Program at Louisiana State University and Chief of Physics at Mary Bird Perkins Cancer Center in Baton Rouge.

Peter R Almond, PhD, DABR, received his undergraduate honours degree in physics from Nottingham University and his training in medical physics from Bristol University. He moved to the United States in 1959 and earned his MS and PhD in physics (nuclear) from Rice University in Houston. From 1964 to 1985, he worked at The University of Texas M D Anderson Cancer Center in Houston, serving as Head of the Radiation Physics Section, Director of the Cyclotron Unit and Professor of Biophysics. From 1985 to 1998, he was Vice Chairman of the Department of Radiation Oncology at the University of Louisville. Dr Almond helped develop cancer treatments with various forms of radiation, including electrons and neutrons. He has also been instrumental in writing dose calibration protocols for photon and electron beams. He served as the North American Editor for *Physics in Medicine and Biology* and was the founding Editor-in-Chief of the electronic *Journal of Applied Clinical Medical Physics*. Dr Almond is a Fellow of the AAPM, ACMP, ACR and IOP and served as AAPM President in 1971. He received the AAPM Coolidge Award and the ACMP Marvin M D Williams Award in 1990. Now retired, he teaches part-time and is writing the early history of the Physics Department at the M D Anderson Cancer Center.